



TECHNISCHE
UNIVERSITÄT
WIEN
Vienna University of Technology

Diplomarbeit

Homo- and Heteronuclear Mn(I) Complexes Based on PN- Ligand Systems

ausgeführt zum Zwecke der Erlangung des akademischen Grades eines

Diplom-Ingenieurs

unter der Leitung von

Univ.-Prof. Dipl.-Ing. Dr. techn. Karl Kirchner

und

Univ.-Ass. Dipl.-Ing. Gerald Tomsu

Univ.-Ass. Dipl.-Ing. Stefan Weber

(E163 Institut für Angewandte Synthesechemie)

eingereicht an der Technischen Universität Wien

Fakultät für Technische Chemie

von

Ines Blaha, BSc

01207428 (066 490)

Brüßlgasse 15-25/22/9

1160 Wien

Wien, im Mai 2021

Ich nehme zur Kenntnis, dass ich zur Drucklegung meiner Arbeit unter der Bezeichnung

Diplomarbeit

nur mit Bewilligung der Prüfungskommission berechtigt bin.

Ich erkläre an Eides statt, dass die vorliegende Arbeit nach den anerkannten Grundsätzen für wissenschaftliche Abhandlungen von mir selbstständig erstellt wurde. Alle verwendeten Hilfsmittel, insbesondere die zugrunde gelegte Literatur, sind in dieser Arbeit genannt und aufgelistet. Die aus den Quellen wörtlich entnommenen Stellen, sind als solche kenntlich gemacht.

Das Thema dieser Arbeit wurde von mir bisher weder im In- noch Ausland einer Beurteilerin/einem Beurteiler zur Begutachtung in irgendeiner Form als Prüfungsarbeit vorgelegt. Diese Arbeit stimmt mit der von den Begutachterinnen/Begutachtern beurteilten Arbeit überein.

Wien, im Mai 2021

Unterschrift

Danksagung

Zunächst möchte ich mich bei Prof. Dr. Karl Kirchner für die Chance bedanken, meine Diplomarbeit in seiner Arbeitsgruppe zu absolvieren.

Großer Dank gilt meinen Betreuern Gerald Tomsu und Stefan Weber für ihre unermüdliche Unterstützung und ihr offenes Ohr. Danke für die lustige Zeit in Labor und Büro, in den gemeinsamen Pausen und für die Aufmunterung, wenn es mal nicht so gut gelaufen ist.

Ganz herzlich will ich mich natürlich auch bei meinen Kollegen aus der Arbeitsgruppe bedanken: Julian Brünig, Wolfgang Eder, Sarah Fleissner, Daniel Himmelbauer, Matthias Käfer, Jan Pecak, Heiko Schratzberger und Daniel Zobernig. Danke für die unglaublich lustige Zeit im Labor und die tollen Abende, an denen ich oft nicht nur sehr viel gelacht, sondern auch noch etwas gelernt habe. Wenn man so herzlich aufgenommen wird wie bei euch, kann man (trotz manchmaliger Nachfrage) vergessen, dass man vielleicht noch gar nicht so lange auf der TU ist.

Ein unglaublich großes Dankeschön gebührt Karl und meiner Mutter, die mich bei jeder meiner Entscheidungen unterstützt haben. Und noch einmal ganz besonders meiner Mutter, die mich überhaupt erst zu einem Menschen gemacht hat, der sich traut, seine eigenen Entscheidungen zu treffen und zu ihnen zu stehen.

Ich möchte mich bei den tollen Menschen bedanken, die mich begleitet und unterstützt haben; bei meiner Familie, wie auch bei denen, die ich in den letzten Jahren kennengelernt habe oder auch schon länger kenne. Vielen Dank für Ermunterung, Ablenkung oder auch einfach das Verständnis, wenn ich keine Zeit hatte insbesondere an Mike, Beni, Benji, Chris, Claudia, Dani, Flo, Steffi aber auch so viele andere. Und Kerstin.

Abstract

The majority of transition metal complexes previously employed for catalytic transformations are based on noble metals. Although these metals display high stability and reactivity, there are disadvantages that have to be considered. Due to high prices and growing supply risks regarding noble metals, earth-abundant transition metals have gained a lot of interest in the last decades.

Alkylated transition metal carbonyls are known for participating in migratory insertion reactions. This type of reaction forms an acyl moiety and at the same time generates a vacant coordination site at the metal center. Therefore, migratory insertion can promote catalytic activity of transition metal complexes.

In this thesis, a pyrimidine-based PN-ligand system was chosen due to its coordination mode. Since the utilized ligand enables formation of binuclear complexes, one coordination site was saturated by introducing chromium, molybdenum or tungsten carbonyls. Coordination of group 6 metals was achieved by reaction of hexacarbonyl precursors with the ligand under solvothermal conditions.

To obtain complexes that may undergo migratory insertion, alkylation of manganese(I) carbonyls was investigated within this thesis. Owing to their reactivity, many common alkylation reagents, including organolithium compounds, participate in side reactions. Therefore, an alternative protocol was studied within this work based on diorganozinc reagents.

Formation of a cationic intermediate was considered to facilitate the alkylation step. Therefore, halide coordinated to manganese(I) had to be substituted. A variety of halide abstraction agents was investigated for this transformation.

Zusammenfassung

Integraler Bestandteil der modernen metallorganischen Chemie ist die Entwicklung neuartiger Katalysatoren für organische Reaktionen. Viele dieser Komplexe basieren auf Platingruppenelemente. Trotz ihrer Reaktivität und Stabilität gibt es Nachteile, die nicht außer Acht gelassen werden sollten. Steigende Rohstoffpreise sowie ein drohender Versorgungsengpass führten in den letzten Jahren zur Entwicklung von Katalysatoren, welche auf unedlen Metallen basieren.

Insertionsreaktionen von Alkylgruppen in Carbonylliganden ist ein Schlüsselschritt in vielen industriellen homogenen Katalysen. Durch Wanderung des Alkylgruppen entsteht eine freie Koordinationsstelle, welche für die Reaktivität der Komplexe verantwortlich ist.

Für diese Arbeit wurde ein PN-Liganden-System gewählt, welches auf Pyrimidin basiert. Da der untersuchte Ligandentyp zwei Koordinationsstellen aufweist, wurde eine mit Chrom-, Molybdän- oder Wolfram- Carbonylen gesättigt. Hierfür wurde der Ligand mit dem jeweiligen Hexacarbonyl-Precursor in einer Solvothermalysynthese umgesetzt.

Um Komplexe zu erhalten, welche Insertionsreaktionen eingehen können, wurde die Alkylierung von Mangan(I)-Komplexen im Zuge dieser Arbeit eingehend untersucht. Die Reaktion mit Organolithium-Verbindungen führte, bedingt durch die hohe Reaktivität dieser Reagenzien, oft zu ungewollten Nebenreaktionen. Im Rahmen dieser Arbeit wurde ein neuartiges Alkylierungsprotokoll, basierend auf Diorganozink-Reagenzien entwickelt.

Der Alkylierungsschritt sollte dabei durch die Bildung eines kationischen Intermediates begünstigt werden, was eine Abspaltung des Halogenid-Liganden vom Mangan-Zentrum erfordert. Zu diesem Zweck wurde eine Reihe unterschiedlicher Reagenzien zur Halogenid-Abstraktion untersucht.

Table of contents

Danksagung	II
Abstract	III
Zusammenfassung.....	IV
Table of contents.....	V
1 Introduction.....	1
1.1 Carbonyl Transition Metal Complexes	2
1.2 Phosphine Ligands	10
1.3 Nitrogen Ligands.....	13
1.4 Manganese(I) Complexes in Catalysis	15
1.5 Alkylation of Transition Metal Complexes	19
2 Aim of the Thesis.....	21
3 Results and Discussion	22
3.1 Synthesis of Ligands.....	22
3.2 Synthesis of Complexes	22
3.3 Alkylation of Complexes	26
4 Conclusion and Outlook	33
5 Experimental Part.....	34
5.1 Materials and Methods	34
5.2 Synthesis of Ligands.....	34
5.3 Synthesis of Complexes	39
5.4 Functionalization of Complexes	49
6 References.....	52
7 List of Abbreviations.....	57

1 Introduction

Developments in the field of catalysis are driven by economic and environmental considerations. One major advantage of catalysis over the use of stoichiometric reagents is minimization of waste. Reducing the amount of undesired byproducts can lower deposition costs and decrease environmental pollution. Moreover, utilization of catalysts allow for lower reaction temperatures and therefore reduce energy consumption.¹

Owing to their reactivity and stability, catalysts based on platinum-group metals (PGMs), like rhodium, palladium and platinum, are widely-used for a variety of chemical transformations. However, low abundance of these metals in the earth's crust and steadily increasing supply risk are major drawbacks that have to be addressed.²

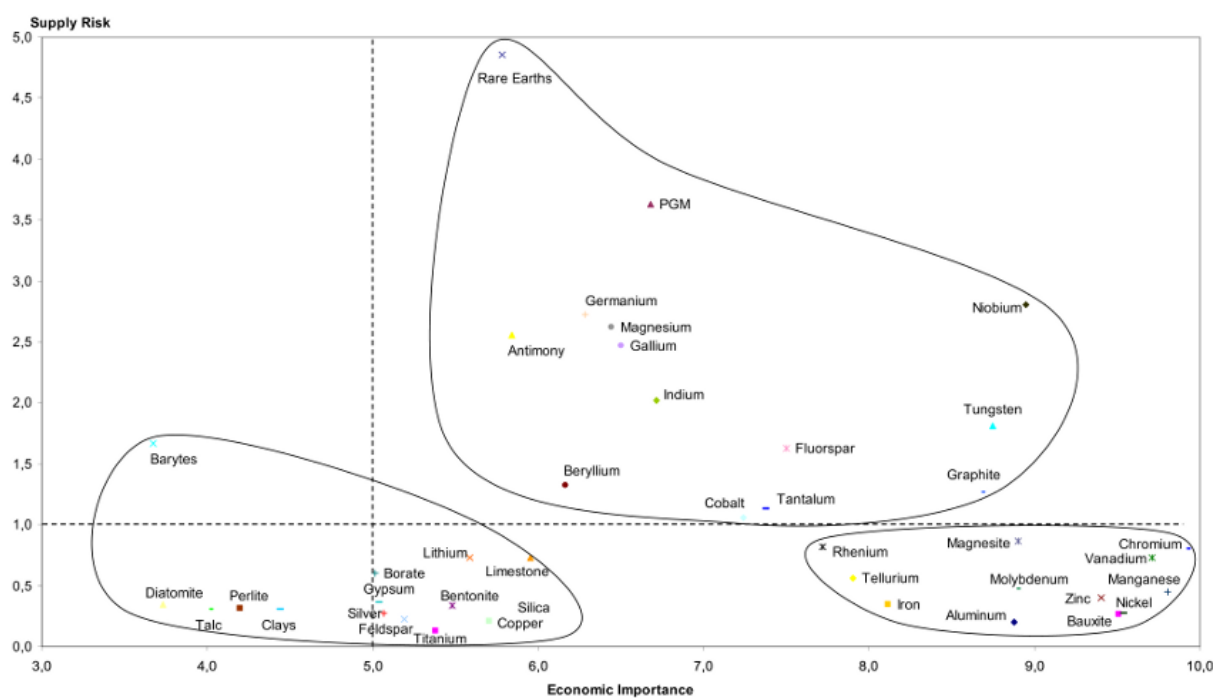


Figure 1 Economic importance and supply risk of raw materials in the EU²

Therefore, a recent trend in the field of catalysis is the replacement of precious metals for more earth-abundant ones, like iron, cobalt and nickel. Another appealing alternative displays manganese, since it is the third most abundant transition metal in earth's crust.³

Upcoming chapters are devoted to common ligands in well-defined manganese(I) catalysts, including carbon monoxide, phosphines and amines. Recent developments in the field of manganese(I)-based redox-catalysis will be covered in Section 1.4.

1.1 Carbonyl Transition Metal Complexes

Carbon monoxide donates a lone electron pair to the metal center forming a σ -bond. However, there are more complex aspects in the nature of CO bonding to a metal center, since it is also capable of accepting electrons.

Backbonding or π -bonding refers to the ability of ligands to accept electrons from a metal center. These electrons are donated into ligand orbitals with π -symmetry, therefore making these kind of ligands π -acceptors. The interaction is based on the overlap of an unoccupied π^* -orbital of the ligand with a filled d-orbital of the metal. The resulting molecular orbital (MO) is lower in energy than the preceding orbitals. The lowering of orbital energy provides additional stability to the formed complex (Figure 2, **a**). If a ligand lacks those π^* -orbitals, as it is the case for NH_3 , no such additionally stabilizing interactions may occur (Figure 2, **b**).⁴

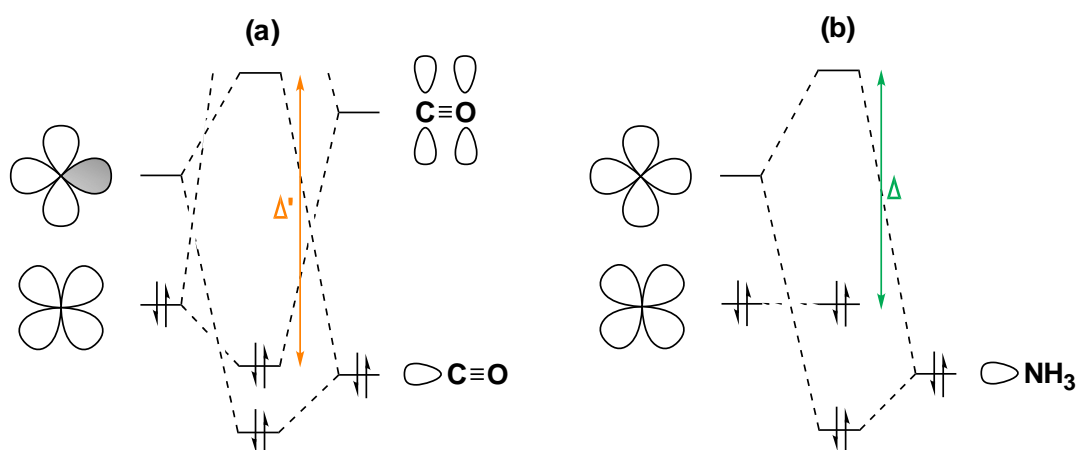


Figure 2 Orbitals involved in M-L-bonds for π -acceptors **a** and σ -donors **b** (Modified based on ⁴)

Furthermore, the lowered orbital energy increases the ligand field splitting energy (LFSE, Δ), which represents the energy gap between the HOMO and the LUMO. If there are no noteworthy π -interactions with suitable ligand orbitals, the metal orbitals with π -symmetry stay unaltered (Figure 2, **b**). However, with π -acceptors the HOMO energy level is lowered.

Carbon monoxide also acts as a Lewis base by donating lone pair σ -electrons from the carbon atom. The reason for the coordination *via* the carbon and not *via* the oxygen lone electron pair is found in the way how a metal-ligand bond is formed. Bond formation is based on the interaction of the metal LUMO with the HOMO of the donating ligand. As oxygen is more electronegative, its orbitals are lower in energy and therefore unavailable for σ -bond formation between carbon monoxide and the metal.⁵

However, σ -donation and π -bonding contribute as synergistic effect. σ -Donation provides electron density to the metal, which can be donated into the π^* -orbital of the CO ligand. At the same time, backbonding is promoted by removing electron density from CO *via* σ -donation.⁵

Ligands capable of backbonding are especially favored for electron-rich metals, since donation into the π^* -orbital decreases electron density of the metal center. Therefore, carbon monoxide forms strong bonds with low-valent transition metals, resulting in many prominent examples such as $\text{Cr}(\text{CO})_6$, $\text{Mo}(\text{CO})_6$, $\text{Fe}(\text{CO})_5$, $\text{Ni}(\text{CO})_4$ or $\text{Mn}(\text{CO})_5\text{Br}$.⁶

Another consequence of backbonding is based on the accepting orbital type π^* . Backbonding weakens the corresponding internal C-O bond and decreases the bond order. Thereby the ability of the coordinated metal atom for backdonation can be monitored by IR spectroscopy. The CO stretching frequency ν_{CO} decreases in value compared to the free gas (Table 1).⁴

Table 1 Examples for CO stretching frequencies in different carbonyl complexes⁷

Compound	ν_{CO} [cm^{-1}]
Free CO	2143
$\text{Mn}(\text{CO})_5\text{Br}$	2036
$\text{Mo}(\text{CO})_6$	2004
$\text{Cr}(\text{CO})_6$	2000
$\text{W}(\text{CO})_6$	1998

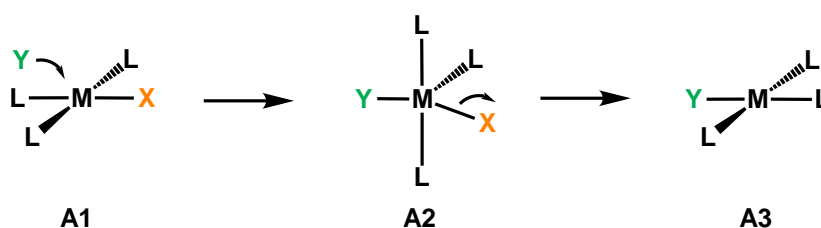
1.1.1 Reactivity of Carbonyl Complexes

Ligand Substitution Reactions

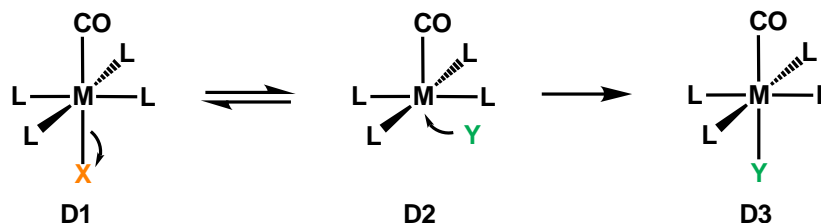
Carbonyl complexes are suitable precursors and therefore regularly participate in ligand substitution reactions. From a thermodynamic view this can be explained by the leaving group properties of CO. As a neutral, stable gas it is easily released compared to hydride or alkyl ligands, which would be extremely unstable in their free form.⁴ However, bond strength also depends on the involved metal. A decrease in bond strength can often be observed when switching from first- to second- and to third-row transition metals.⁶

Ligand substitution reactions can be divided into two major types: the associative and the dissociative mechanism (Scheme 1). They may be compared to related nucleophilic substitution pathways $\text{S}_{\text{N}}1$ and $\text{S}_{\text{N}}2$ in organic chemistry.

Associative:



Dissociative:



Scheme 1 Associative and dissociative mechanisms of ligand substitution

Associative ligand substitution is common for square planar $16e^-$ complexes **A1** (Scheme 1, top). It is initiated by the attack of the nucleophile **Y**. Therefore, involved complexes are usually coordinatively unsaturated. The rate-determining step is the entering of the new ligand **Y**, while the influence of the dissociating ligand **X** on the overall reaction rate is weak.

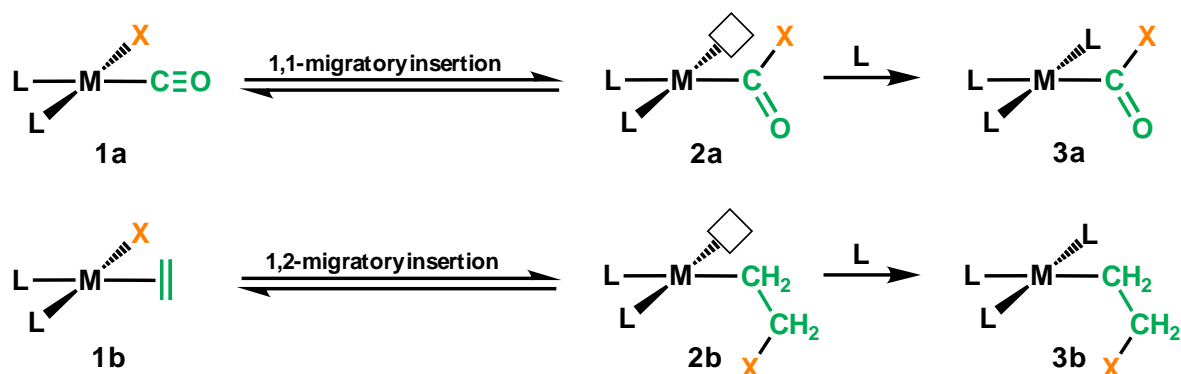
As carbonyls are often coordinatively saturated $18e^-$ complexes **D1** (Scheme 1) their preferential mode for ligand substitution is the dissociative mechanism. It is characterized by the initial M-L-bond cleavage, which is the rate-determining step. This step is determined by an equilibrium of **D1** and **D2**. Upon dissociation of a ligand, an unsaturated $16e^-$ complex **D2** is formed that can bind an incoming ligand.⁴

Apart from coordinative saturation there are other factors favoring a dissociative mechanism such as sterical hinderance of the metal center by bulky ligands and electronic effects of co-ligands. One of these effects is the structural *trans* effect also referred to as *trans* influence. It is strong for π -acceptors like carbon monoxide and results in a weakened bond of ligand **X** (Scheme 1) *trans* to it. This is caused by electronic effects including polarization. Strong π -acceptors will avoid a position in the plain of the square-pyramidal intermediate **D2** and therefore promote elimination of a ligand *trans* to them.⁸

Migratory Insertion

Migratory insertion is a key step in many catalytic cycles. Two types of this reaction pattern can be described (Scheme 2). With ligands coordinated end-on **1a** 1,1-insertion proceeds. In

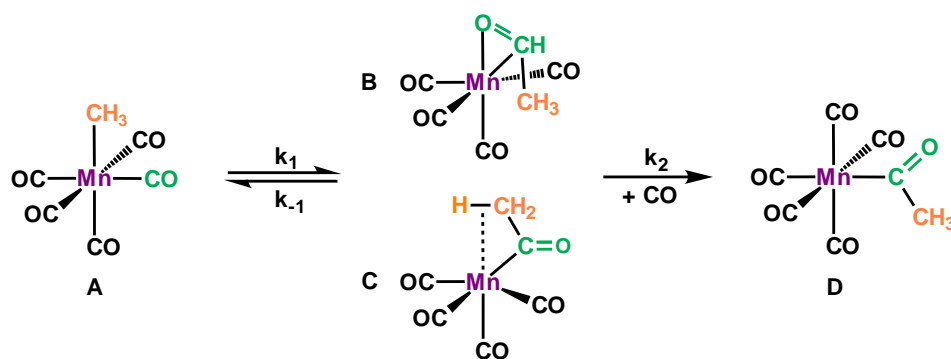
the obtained product **3a** the metal and the former anionic ligand X are bound to the same atom. With ligands coordinated side-on **1b** 1,2-insertion occurs.⁵



Scheme 2 Types of migratory insertion⁹

Upon migration the anionic ligand X leaves a vacant site forming an unsaturated complex lacking two electrons **2a**, **2b**. Afterwards the unsaturated intermediate binds an incoming neutral ligand L yielding a saturated complex **3a**, **3b**.¹⁰

The mechanism of migratory insertion has been extensively studied on the basis of $\text{MeMn}(\text{CO})_5$ (Scheme 3).^{10,11} While migration of the alkyl group to CO and *vice versa* seemed possible, migration of the alkyl moiety turned out to be the more common.¹² Regarding the structure of the intermediate **2a** (Scheme 2), stabilization by the acyl-O occupying the vacant site seems plausible. This structure is known for some acyl complexes of precious metals, e.g. rhodium.¹³ Cryogenic studies indicated a η^1 coordinated acyl in the intermediate Mn complexes.¹⁴ However, computational studies propose two possible intermediates. Species **B** (Scheme 3) with the acyl-O bound to Mn^{15} or species **C** stabilized by a C–H–agostic interaction¹⁶.



Scheme 3 Migratory insertion on $[\text{MeMn}(\text{CO})_5]$

Kinetic studies¹¹ proposed a two-step mechanism of migratory insertion. Kinetics of the overall process can be considered first order, second order or mixed. The observed order depends on the ratio of reaction rates for the migration step, the reversal of migration and coordination of the new ligand. For $\text{MeMn}(\text{CO})_5$ (Scheme 3) with high CO partial pressure the rate of the ligand uptake k_2 , yielding the saturated product **C**, is fast. In comparison, the rate k_{-1} of the intermediate $[(\text{RCO})\text{-Mn}(\text{CO})_4]$ **B** transforming back into **A** is negligible. The reaction is zero order in CO and overall first order. For lower carbon monoxide partial pressure the reaction rate is a function of the CO concentration and overall second order.¹²

In contrast, reaction rates of $\text{PhMn}(\text{CO})_5$ are independent from CO concentration. The overall reaction rate is dominated by the formation rate of the acyl complex $[(\text{PhCO})\text{-Mn}(\text{CO})_4]$.¹² This fact hints to the influence of the electronic nature of the hydrocarbon moiety. Electron-withdrawing properties stabilize the existing metal-carbon bond and destabilize the newly formed carbon-carbon bond upon migration.⁴ Therefore, carbonylation rates are decelerated for these moieties and migratory aptitudes in $\text{RMn}(\text{CO})_5$ follow the trend: $n\text{Pr} > \text{Et} > \text{Me} > \text{CH}_2\text{Ph}$.¹²

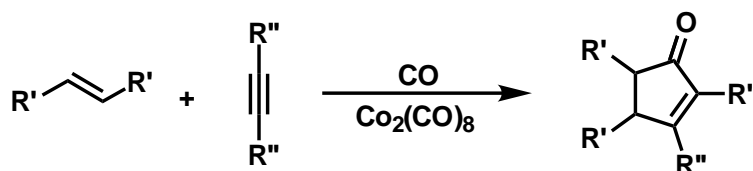
Migratory insertion can be accelerated upon Lewis acid catalysis. Coordination of Lewis acid to the carbonyl oxygen is stronger for the acyl group than for carbon monoxide. This might be an additional driving force. For $\text{MeMn}(\text{CO})_5$ protic acids like dichloroacetic and trifluoroacetic acid were found to enhance reaction rates. Furthermore, the effect increases with the strength of the acid.¹⁷ Another condition influencing insertion reaction rates is the solvent. Migratory insertion rates tend to increase in polar solvents, although the origin of this effect is hard to generalize.⁴

1.1.2 Applications of Carbonyl Complexes

Carbonyl complexes are used in a multitude of reactions. The Pauson-Khand reaction will be outlined as an example for stoichiometric use. In contrast, hydroformylation and Monsanto's acetic acid process display catalytic performances of Co and Rh carbonyl species.

Pauson-Khand Reaction

The Pauson-Khand reaction (Scheme 4) enables the synthesis of α,β -unsaturated cyclopentenones. Thereby an alkyne and an alkene react with carbon monoxide in a [2+2+1]-cycloaddition.¹⁸ The original procedure utilized $\text{Co}_2(\text{CO})_8$ and was discovered by Khand in the 1970s, but some drawbacks had to be overcome. The original method required harsh conditions and gave rather low yields.¹⁹

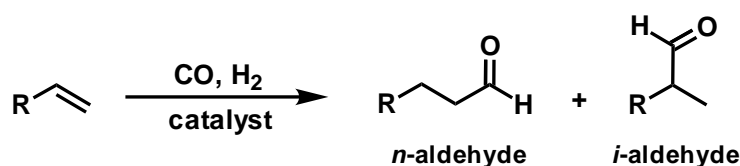


Scheme 4 Pauson-Khand reaction

Addition of *N*-oxides and sulfoxides led to milder reaction conditions and shorter reaction times.²⁰ Approaches to avoid the formation of metal clusters or inactive species, which was found to be the main reason for the demand of stoichiometric amounts, were the addition of phosphites ($\text{P}(\text{OR})_3$) and phosphines (PR_3) as co-ligands.²¹

Hydroformylation

Upon hydroformylation an alkene is prolonged by one carbon atom due to addition of carbon monoxide. It is one of the most important homogeneously catalyzed reactions in chemical industry, producing aldehydes that can be processed into alcohols, acids and amines.⁴



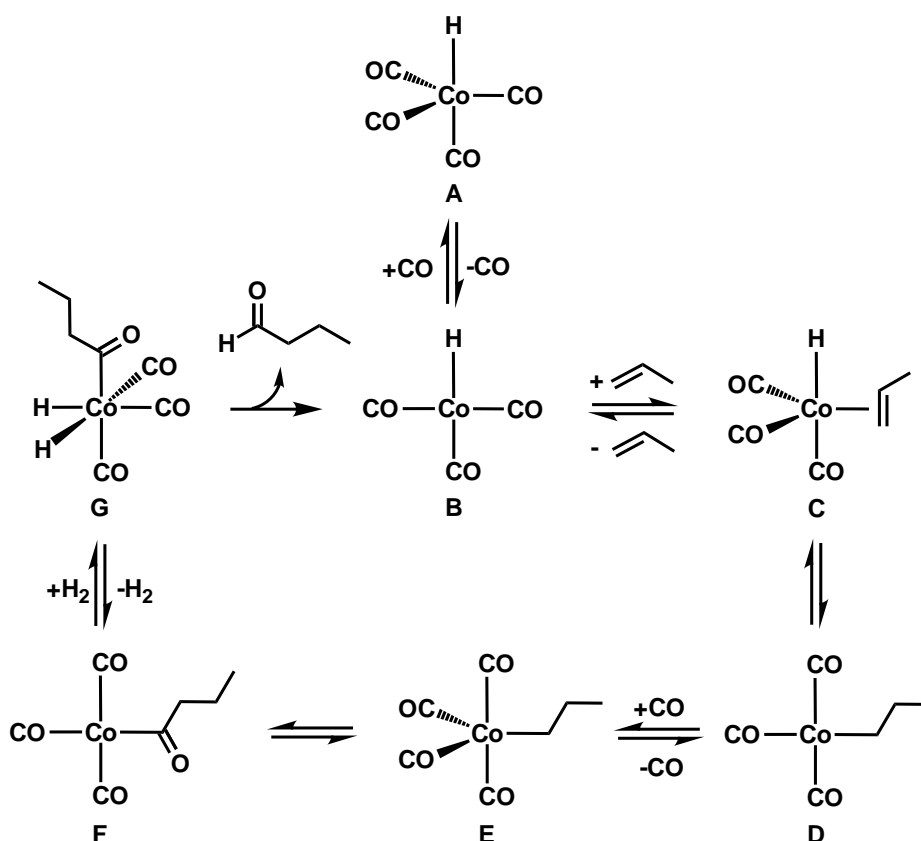
Scheme 5 Alkene hydroformylation²²

The first transition metal complex applied as catalyst for hydroformylation was $\text{Co}_2(\text{CO})_8$. Formation of $\text{HCo}(\text{CO})_4$ by addition of H₂ initiates the catalytic cycle. Later modifications such as addition of phosphine ligands (PR_3) increased the yield of commercially favored *n*-aldehyde.

Additionally, lower CO pressure and higher temperatures without decomposition of the catalyst were observed. With $\text{HCo}(\text{CO})_3\text{PR}_3$ being capable of alkene isomerization even internal alkenes could be converted into linear aldehydes at maintainable reaction conditions.²³

The catalytic cycle of hydroformylation (Scheme 6) was investigated by Heck and Breslow²⁴. It consists of formation of a vacant site on the catalyst by loss of one molecule CO to give **B**. Alkene is coordinated side-on to complex **C**, donating two electrons from its C–C double bond. The alkene is converted to an alkyl ligand **D** by insertion into the metal-hydride bond. An acyl moiety is formed by a consecutive migration step from **E** to **F**. Oxidative addition of H_2 generates two hydrides **G** followed by reductive elimination of aldehyde.

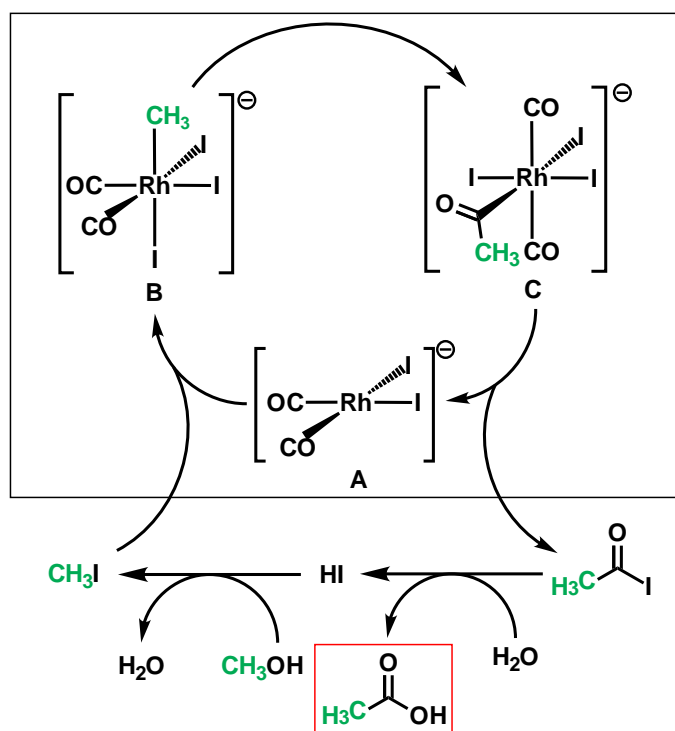
The process was further improved by employing Rh-based catalysts. Presence of PPh_3 led to the formation of the catalytically active species $\text{HRh}(\text{CO})(\text{PPh}_3)_2$. Hydroformylation at room temperature and atmospheric pressure yielded aldehydes in the ratio of about 20:1 (*n*:*i*).²⁵



Scheme 6 Simplified mechanism of hydroformylation reactions²⁴

Monsanto's Acetic Acid Process

Another carbonyl centered process of industrial importance is Monsanto's acetic acid process, a carbonylation reaction of methanol. It was first discovered using cobalt as catalyst and later refined by Monsanto with the application of Rh-based catalysts enabling lower temperatures and significantly lower pressure.⁴



Scheme 7 Mechanism of Monsanto's acetic acid process²⁶

The active species is rhodium catalyst **A** (Scheme 7) bearing iodine and carbon monoxide ligands. Upon reaction with HI, methanol is transformed into iodomethane. This newly formed CH_3I then enters the Rh-cycle and undergoes oxidative addition to give $[\text{MeRh}(\text{CO})_2\text{I}]^-$ **B**. Migratory insertion of the methyl group to CO forms an acyl moiety and the vacant position is filled by CO **C**. Reductive elimination releases acetyl iodide which is transformed into acetic acid by reaction with water. The recovered Rh catalyst is able to enter a new catalytic cycle.²⁶

1.2 Phosphine Ligands

Phosphines are frequently encountered as ligands in transition metal complexes. Due to high variability this ligand class is able to stabilize transition metals in different oxidation states. Interaction of phosphine ligands with a transition metal center occurs by σ -donation of the electron pair of the phosphorous atom. Apart from that, backbonding is possible. Due to the lack of π^* -orbitals, metal electrons are accepted by the P-R σ^* -orbital.⁴

By contribution of the moiety R to the P-R σ -bond, backbonding is facilitated. This electronic influence was investigated by Tolman using CO stretching frequencies for quantification (Table 2). Comparing ν_{CO} values in $[\text{Ni}(\text{CO})_3\text{PR}_3]$ the strongest donation and least backbonding was observed for P^tBu_3 . In comparison, phosphites ($\text{P}(\text{OR})_3$) and PF_3 show the least effective donation to the metal.²⁷

Table 2 ν_{CO} -Values for different phosphorous ligands²⁷

Ligand	ν_{CO} [cm^{-1}]
P^tBu_3	2056
PMe_3	2064
PPh_3	2069
$\text{P}(\text{OMe})_3$	2079
PF_3	2110

Other aspects of phosphine ligand properties are steric effects. A quantifiable value is the cone angle θ , enclosed by the metal atom and the outer boundaries of the phosphine moieties R (Figure 3). Its value indicates the binding ability of phosphine ligands to a metal center and is therefore essential for the later reactivity of the formed complex. For example, the tendency for phosphines to dissociate from a palladium metal center is $\text{P}^i\text{Pr}_3 > \text{PPh}_3 > \text{PEt}_3 > \text{PMe}_3$. Values for an investigated Ni(0) complex show a resemblance to that. The decrease in binding ability could not be explained satisfyingly by electronic properties alone. In fact, it was found to correlate with the cone angle. This can be explained with increasing congestion around the phosphorous atom aggravating the formation of a strong P-M bond. Nevertheless, there are some limitations to this concept.²⁷

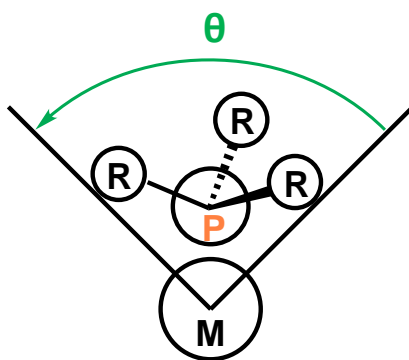


Figure 3 Graphic illustration of the cone angle θ (Modified based on ²⁷)

Electronic and steric parameters are closely affiliated with each other and cannot be seen as an independent parameters. Therefore they are plotted in Tolman maps (Figure 4).²⁷

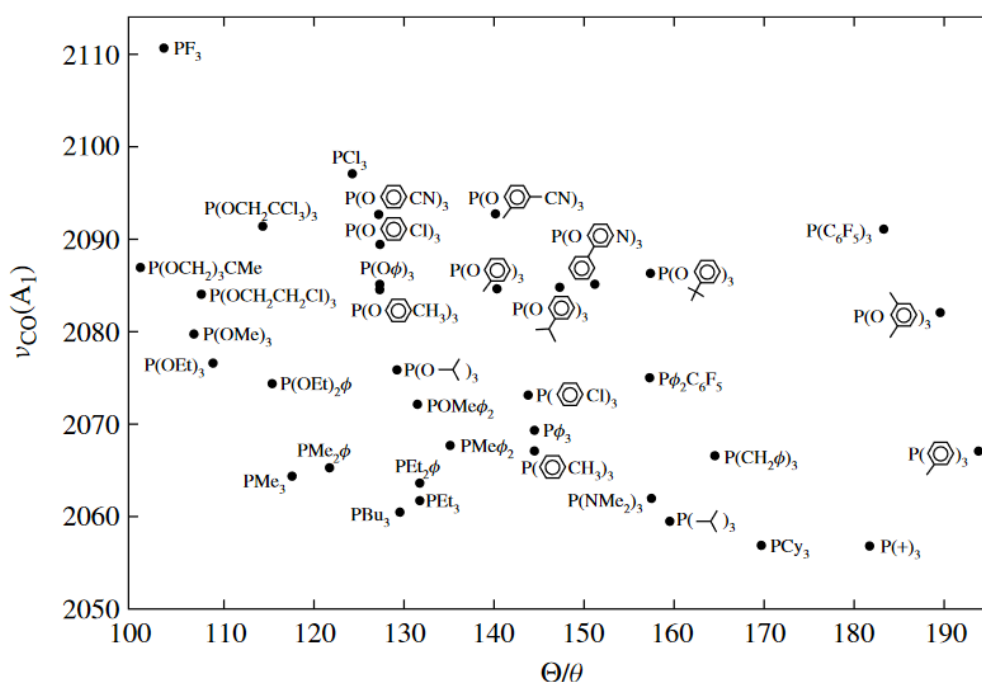


Figure 4 Tolman map of steric (θ) and electronic (ν_{CO}) effects⁵

It is the combination of properties making phosphines play a major role as ligands in homogenous catalysis. Many prominent examples for homogenous catalysts are based on this ligand class. These examples include Vaska's compound, an Ir(0) complex crucial for the early studies of oxidative addition²⁸, as well as Wilkinson's catalyst widely used for hydrogenation of alkenes (Figure 5).²⁵

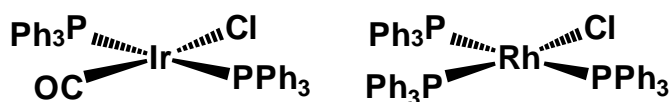


Figure 5 Vaska's complex and Wilkinson's catalyst

1.2.1 Bisphosphines

A frequently encountered arrangements of phosphine ligands are those binding to a metal atom by more than one phosphorous atom. These types of ligands increase the stability of the complex by the chelate effect. Chelate ligands replace comparable monodentate ligands more easily, since entropy increases. If one M-L bond to the chelate ligand is broken the remaining bonds keep the ligand in close proximity to the metal center. Reoordination of the chelate ligand is therefore facilitated.

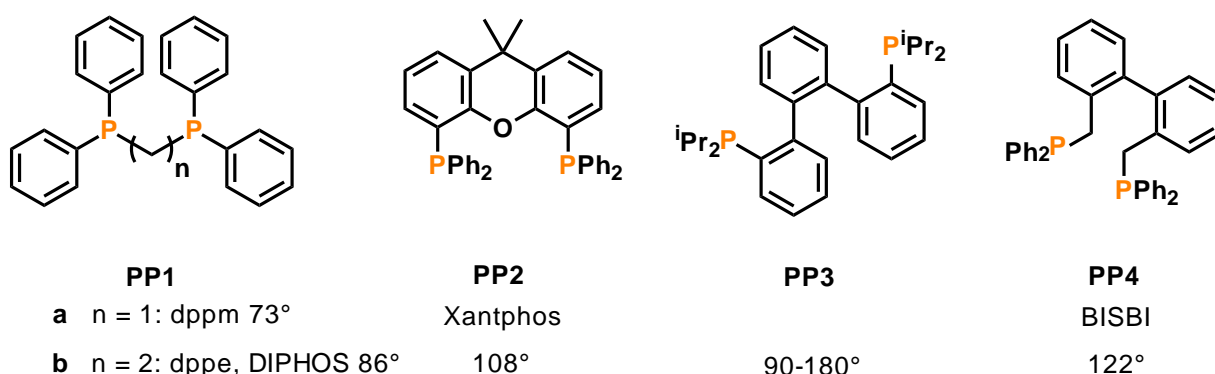


Figure 6 Examples on different bisphosphines and their bite angles

Similar to monodentate phosphines there is a quantifiable parameter describing the binding mode to a transition metal, which represents the bite angle. Phosphines with different structures enforce their assembly in different conformations (Figure 6). The backbone distance between the phosphorous atoms often affects preferred bite angles, e.g. for dppm **PP1a** and dppe **PP1b**.⁴ However, phosphines with elonged P-P backbone distances can be very flexible, like **PP3**, which can adapt bite angles between 90° and 180°.⁵

The bite angle is a parameter heavily influencing the reactivity and selectivity of a complex. Phosphines with wide bite angles can promote the formation of certain complex geometries. Therefore, these ligands can facilitate crucial catalytic steps. Application of different bisphosphines in C-C and C-X coupling reactions has been reviewed by van Leeuwen and co-workers.²⁹ Ni(II) complexes bearing bisphosphines of the xantphos type **PP2** were found to be active hydrocyanation catalysts.³⁰ The wide bite angle of this ligand type facilitates reductive elimination by destabilizing the square planar Ni(II) and stabilizing the resulting Ni(0) species. Moiseev and co-workers³¹ demonstrated the influence of bite angles on Pd-catalysts employed in the arylation of methyl acrylate. Diphos **PP1b** with a bite angle of 86° led to a stable and therefore catalytically inactive species. In contrast, deviating bite angles, like 73° for dppm **PP1a**, gave a pre-catalyst that was able to form an active species.

In hydroformylation processes Rh complexes bearing a BISBI ligand **PP4** proved to be valuable due to increasing the yield of *n*-aldehyde.³² With bisphosphines of the Xantphos type **PP2** the formation of the desired *n*-aldehyde could be increased by interaction of the ligand in the olefin migration step.²²

1.3 Nitrogen Ligands

Apart from the possible lone pair donation, nitrogen donor atoms differ substantially from phosphorous donors regarding their stereo-electronic properties. Nitrogen can be classified as hard Lewis-base and is therefore not considered as an ideal match for low-valent transition metals. Moreover, tertiary amines are sterically more demanding than comparable trialkyl phosphines. The nitrogen donor bulkiness can again be quantified using cone angle values (Table 3) and is amplified by significantly shorter N-C bonds compared to P-C bonds.⁴

Table 3 Comparison of cone angles for amines and phosphines

R	NR ₃ cone angle θ [°] ³³	PR ₃ cone angle θ [°] ²⁷
Me ₃	132	118
Et ₃	150	132
Ph ₃	166	145

N-heterocyclic compounds, like pyridine, are capable of backbonding to accept electron density from electron rich transition metal centers.³⁴ The switch from monodentate pyridine to bipyridine **NN1** (Figure 7) enhances the stability of the resulting complex due to chelate effect. Backbonding into the π^* -orbitals is strengthened, since the orbitals are lowered in energy due to increased delocalization.

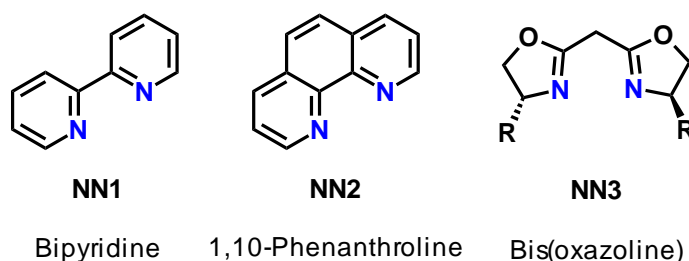
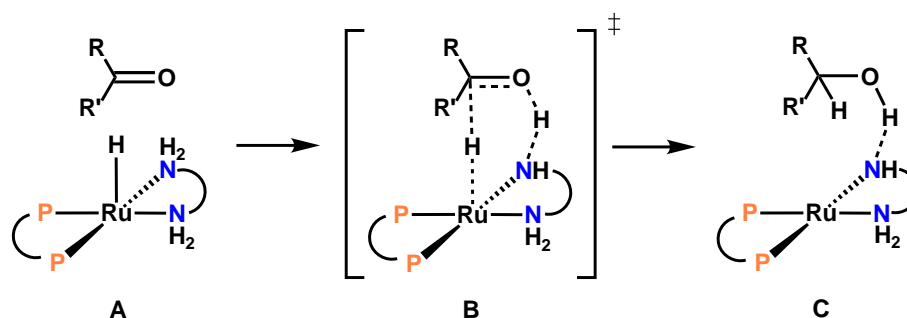


Figure 7 Examples for bidentate *N*-heteroarene ligands

Chelating *N*-heteroarenes (Figure 7), including bipyridine **NN1**, phenanthroline **NN2** and bis(oxazolines) (BOX) **NN3**, are common ligands for the synthesis of *C*₂-symmetric complexes and applications in enantioselective catalysis have been reported.³⁵ BOX ligands have shown

high reactivity in Ir-catalyzed asymmetric reduction of alkyl- and arylketones by transfer hydrogenation using *i*PrOH.³⁶

Noyori and co-workers³⁷ pointed out the crucial role of diamines in the hydrogenation of arylketones. This is attributed to metal-ligand bifunctional catalysis (Scheme 8). As the ketone approaches, a six-membered transition state **B** is formed. Simultaneous transfer of hydride and proton from the amine ligand yield the alcohol forming a hydrogen bond to the anionic amido ligand **C**. Later on, Ru-based systems performed well in reduction of challenging substrates, e.g. 1,2-diaminocyclohexane system capable of reducing esters.³⁸



Scheme 8 Metal-ligand bifunctional catalysis (Modified based on ⁵)

PN-bidentate ligands combine unique reactivities of phosphorous and nitrogen donors and have been studied extensively.³⁹ Phosphorous is able to form strong bonds with late transition metals and backbonding to σ^* -orbitals of phosphines stabilizes low-valent metals. At the same time, N-coordination provides electron density to the metal by σ -donation. This combination of properties enables PN-ligands to form catalytically active species with a broad variety of transition metals in different oxidation states.²⁷

One of the first catalysts bearing PN-ligands was presented by Rautenstrauch and co-workers (Figure 8).⁴¹ Similar to previous systems the complex was based on Ru(II) however, hydrogenation catalysts up to this point included either P–P⁴² or N–N⁴³ ligands. The new catalysts of the general formula $[\text{RuX}_2(\text{P–N})_2]$ and $[\text{RuX}_2(\text{P–N})(\text{P–P})]$ ($\text{X} = \text{H}, \text{Cl}$) display high efficiency for the hydrogenation of ketones and aldehydes. Later, Saudan and co-workers⁴⁴ presented Ru(II) complexes showing high catalytic activity even in the more challenging field of ester hydrogenation to yield alcohols. Moreover, Ru catalysts bearing P–P, N–N or both ligands were found to be inefficient for this transformation.

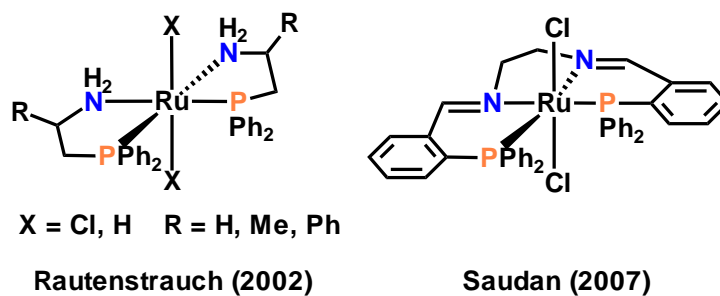
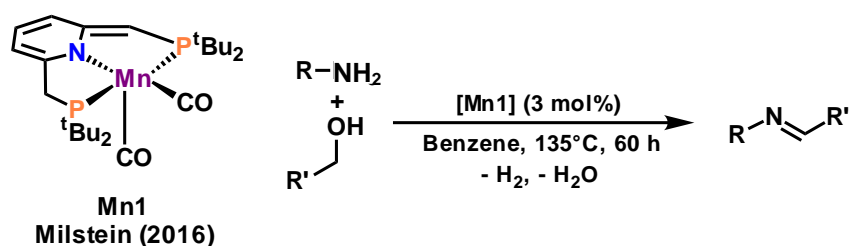


Figure 8 Catalysts based on PN ligands

1.4 Manganese(I) Complexes in Catalysis

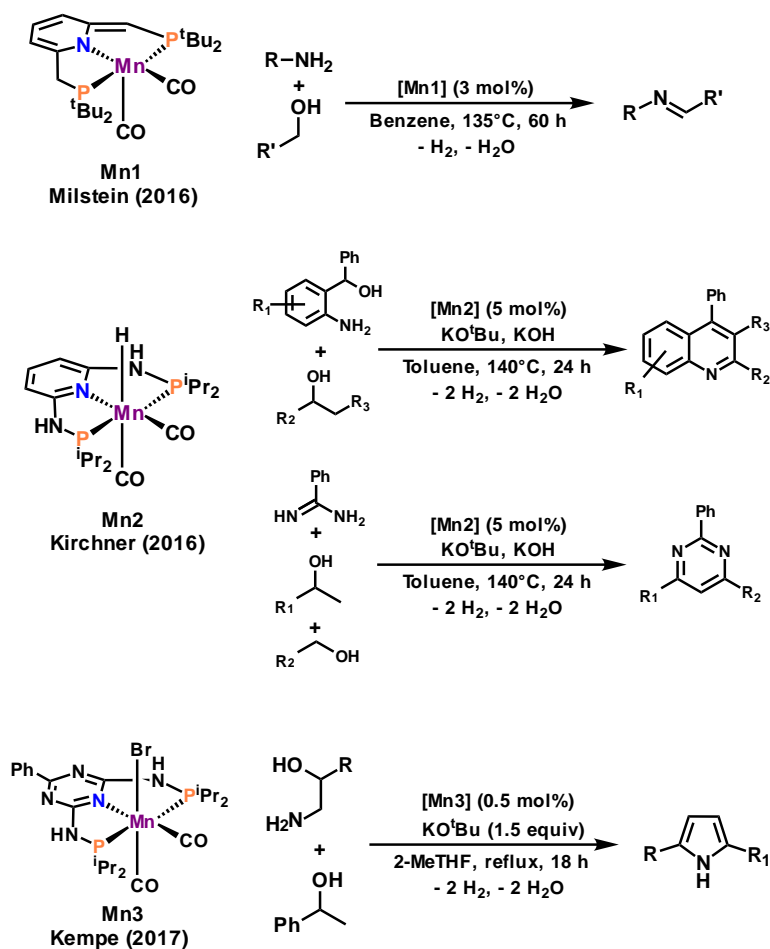
Manganese catalysts have been utilized for a variety of transformations. Hydrogenation and dehydrogenation reactions are two important categories in the field of transition metal catalysis and a selection of suitable Manganese(I) catalysts shall be described in this chapter.

In acceptorless dehydrogenation, alcohols are used as an alkyl source for the alkylation of amines. An imine is formed by reaction of an amine with the carbonyl group obtained by alcohol oxidation. Hydrogen gas and water are the only byproducts.



Scheme 9 Dehydrogenative coupling catalyzed by Mn1

In 2016, Milstein and coworkers⁴⁵ reported on the dehydrogenative coupling of aliphatic and aromatic amines with benzylic alcohols (Scheme 9). The protocol utilized the unsaturated complex **Mn1** bearing a PNP pincer ligand without addition of a base.



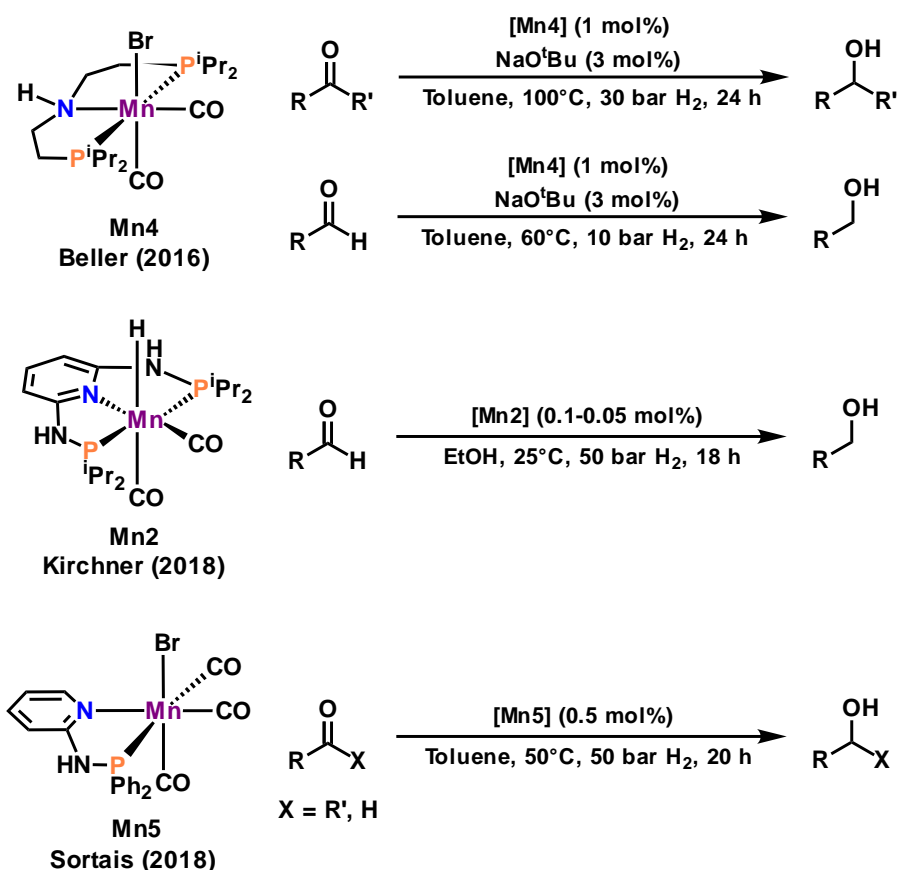
Scheme 10 Synthesis of *N*-heterocyclic compounds catalyzed by **Mn2** and **Mn3**

Acceptorless dehydrogenation can be utilized as a catalytic route for the synthesis of *N*-heterocyclic compounds. The research group of Kirchner⁴⁶ described the synthesis of quinolines from alcohols and 2-amino benzyl alcohol with 5 mol% of hydride complex **Mn2** (Scheme 10). The catalyst was also utilized for the three-component synthesis of pyrimidines. Unfortunately the coupling reactions required stoichiometric amounts of base.

In 2017, Kempe and coworkers⁴⁷ reported the synthesis of functionalized pyrroles from 1,2-aminoalcohols and a variety of secondary alcohols (Scheme 10). Upon addition of 1.5 mol% KO^tBu catalyst **Mn3** bearing a triazin PNP ligand showed good performance, while related Co- and Fe-systems were found to be inactive.

1.4.1 Hydrogenation Reactions

Hydrogenation displays a highly atom efficient way of reducing carbonyl compounds. In addition, hydrogen gas is an inexpensive hydrogen source.⁴⁸ Owing to these facts, there is great interest in developing and improving suitable catalysts for this type of reactions.

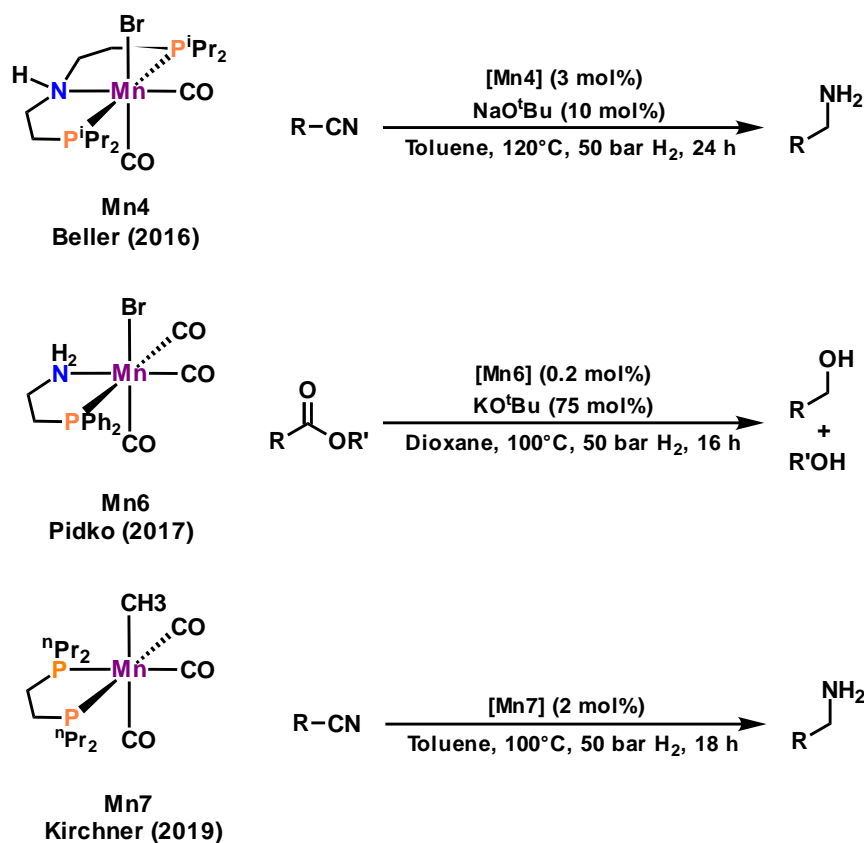


Scheme 11 Hydrogenation reactions catalyzed by **Mn4**, **Mn2** and **Mn5**

In 2016, Beller and coworkers⁴⁹ were the first to report the use of a tridentate Mn(I) catalyst **Mn4** for the hydrogenation of aldehydes and ketones (Scheme 11). Transformations to the corresponding alcohols were performed by 1 mol% catalyst and 3 mol% base. Other functional groups prone to reduction, like C-C double bonds, were tolerated.

The research group of Kirchner⁵⁰ described the chemoselective hydrogenation of aldehydes by a Mn(I) hydride bearing a pyridine-based PNP ligand **Mn2** (Scheme 11). Reduction was conducted at room temperature with merely 0.05 mol% catalyst and without the use of additives. The procedure displayed high chemoselectivity by tolerating C-C double bonds, acetals and even ketones.

In 2018, Sortais and coworkers⁵¹ reported on the hydrogenation of aldehydes and ketones using a manganese(I) complex based on a bidentate ligand system (Scheme 11). **Mn5** showed good performance at 0.5 mol% catalyst loading in the presence of 2 mol% KHMDS. In contrast to a tridentate complex previously synthesized by the group of Sortais⁵² a significant increase in activity could be demonstrated. Comparable results were obtained for the bidentate system at milder reaction conditions.



Scheme 12 Hydrogenation reactions catalyzed by **Mn4**, **Mn6** and **Mn7**

Mn4 was previously demonstrated by Beller and coworkers in the hydrogenation of aldehydes and ketones. Upon increasing the amounts of catalyst to 3 mol% and base to 10 mol% the challenging reduction of nitriles to amines could be achieved. Substrates included (hetero)aromatic- and aliphatic-nitriles as well as dinitriles (Scheme 12).⁴⁹

Catalyst **Mn6** based on a bidentate ligand was described by Pidko and coworkers for the reduction of esters.⁵³ Transformation of aliphatic and aromatic esters into alcohols were achieved at a catalyst loading of solely 0.2 mol%, but unfortunately required 75 mol% of KO^tBu.

The research group of Kirchner⁵⁴ reported on the hydrogenation of various nitriles using the PP-based system **Mn7**. Remarkably, reduction to amines was performed additive-free and with 2 mol% catalyst loading. Additionally, hydrogenation of ketones⁵⁵, alkenes⁵⁶ and carbon dioxide⁵⁷ can be achieved by employing related complexes. Included DFT calculations proposed a mechanism involving migratory insertion for generating the active species. So far, the alkylation protocol for these bisphosphine complexes involved reduction with sodium-potassium alloy and subsequent treatment with organic halides.^{54,55}

1.5 Alkylation of Transition Metal Complexes

Alkyl transition metal complexes are of crucial importance for a multitude of catalytic processes.⁵ Transmetalation is a common way of alkylating transition metals. For successful transmetalation the alkyl donating metal should be significantly more electropositive than the target transition metal. Therefore, organolithium, organomagnesium and organozinc reagents are widely employed.⁵⁸⁻⁶⁰

However, organolithium and organomagnesium compounds display significant reduction potential. One example is the synthesis of ferrocene by Kealy and Pauson.⁶¹ In the attempt to synthesize fulvalene, FeCl_3 was treated with an excess of Grignard reagent CpMgBr . Reduction of the iron salt yielded ferrocene. Similarly, organolithium compounds can act as reducing agents. By treatment of FeCl_3 with MeLi formation of FeCl_2 was observed.⁶² However, reduction is undesired in many cases. Since it is less common for organozinc compounds they appear to be a suitable alternative.

Owing to significant differences in electronegativity between the metal and the carbon atom (Table 4), organolithium and organomagnesium reagents display high reactivity. Attack on other ligands present in a complex is a known adverse effect. The electrophilic carbon atom in carbon monoxide is especially prone to this kind of attack. Increased backbonding by the metal center increases carbon electrophilicity and therefore facilitates the adverse reaction.⁶³

Table 4 Comparison of electronegativity differences in selected metal-carbon bonds⁶⁴

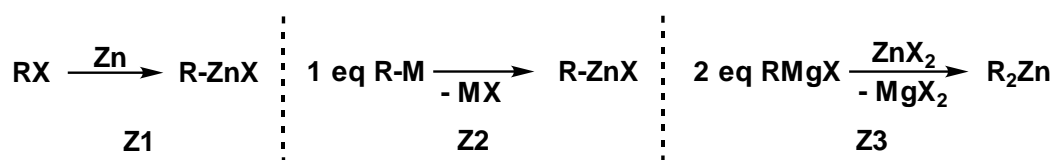
M-C	Electronegativity difference
Li-C	1,57
Mg-C	1,24
Zn-C	0,90

Since the difference in electronegativity between zinc and carbon is considerably smaller than for lithium or magnesium, the Zn-C bond has more covalent character and is less polarized (Table 4). This effect causes the carbon atom to be less nucleophilic. Therefore the reagent can be considered as mild compared to organolithium compounds or Grignard reagents.⁶⁵

Zinc reagents can be divided into three main categories: organozinc halides (RZnX), diorganozincs (R_2Zn) and triorganozincates (R_3ZnM , $\text{M} = \text{Li}, \text{Mg}$). Organozinc halides tend to form halogen bridges and the resulting oligomeric compounds are the most stable and

convenient class of organozinc reagents. In contrast, monomeric diorganozincs are typically volatile and pyrophoric liquids.

For preparation of organozinc halides (Scheme 13), zinc is usually inserted into an organic halide, comparable to the formation of a Grignard reagent **Z1**. Similar to Grignard reactions, the metal needs to be activated. This is usually accomplished by use of a zinc-copper alloy or the even more reactive Rieke zinc. A different approach is treatment of anhydrous zinc halogenides ZnX_2 with organolithium compounds **Z2**. Diorganozincs are usually prepared by the reaction of $ZnBr_2$ with organomagnesium halides **Z3**. The liquid product can be purified by distillation, although this is feasible only for alkyl moieties up to hexyl. Other possible ways are exchange reactions on organic halides or organoboranes with Et_2Zn .⁶⁵



Scheme 13 Preparation of organozinc compounds

Organozinc reagents are capable of transmetallation reactions involving a wide scope of transition metals. In the 1970's the alkylation of tantalum and niobium with diorganozincs was investigated. The methyl metal halides $MeMCl_4$ ⁶⁶, Me_2MCl_3 ⁶⁷ and Me_3MCl_2 ⁶⁷ (M = Ta, Nb) were obtained by the reaction of Me_2Zn with the respective pentachloride MCl_5 . A similar procedure using bis(neopentyl)zinc led to the formation of tris(neopentyl) tantalum dichloride $[(Me_3CCH_2)_3TaCl_2]$.⁶⁸

Regarding organic synthesis, functional group tolerance is one of the most remarkable properties of organozinc compounds, since it leaves ubiquitous functional groups, e.g. esters and nitriles untouched. This makes organozinc compounds valuable reagents for a variety of reactions, such as palladium-mediated Negishi cross-coupling reactions.⁶⁹

2 Aim of the Thesis

The aim of this thesis was the investigation of alkylation procedures for transition metals complexes. Alkylation of carbonyl complexes enables migratory insertion, which generates a vacant site at the metal center. Therefore, it may provide catalytic activity.

Within this thesis, catalytically active Mn(I) complexes bearing an alkyl ligand should be expanded to PN ligand systems. The investigated PN ligands were based on a pyrimidine scaffold. Since these systems feature two coordination sites, combination of manganese(I) with other transition metals was examined (Figure 9).

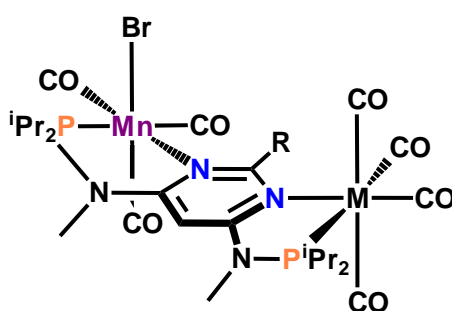


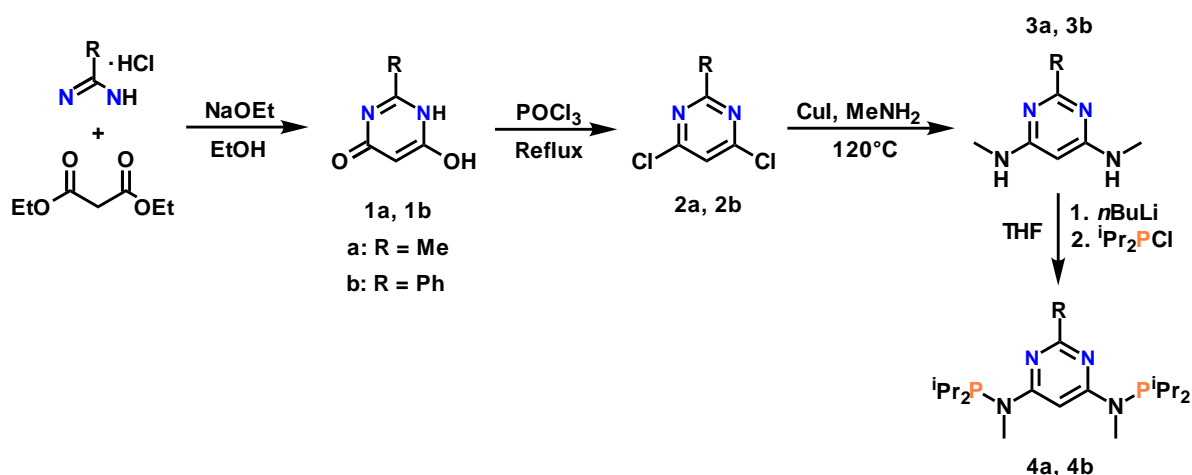
Figure 9 Structure of the synthesized binuclear complexes

Studies towards a general route for the alkylation of a variety of homo- and heteronuclear complexes should be provided. First observations including reduction with Na/K and consecutive alkylation using an alkylhalide as well as the direct treatment of the halide precursor with organolithium reagents should be made. The role of halide abstracting agents in combination with organozinc reagents shall be part of further investigations.

3 Results and Discussion

3.1 Synthesis of Ligands

Two pyrimidine compounds bearing phosphorous groups were chosen as ligands. Both ligands were synthesized utilizing similar procedures (Scheme 14). Starting from acetamidine hydrochloride to obtain *N4,N6*-Bis(diisopropylphosphino)-*N4,N6,2*-trimethylpyrimidine-4,6-diamine (Me-Pyrim) **4a** and starting from benzamidine hydrochloride for *N4,N6*-Bis(diisopropylphosphino)-*N4,N6*-dimethyl-2-phenylpyrimidine-4,6-diamine (Ph-Pyrim) **4b**.



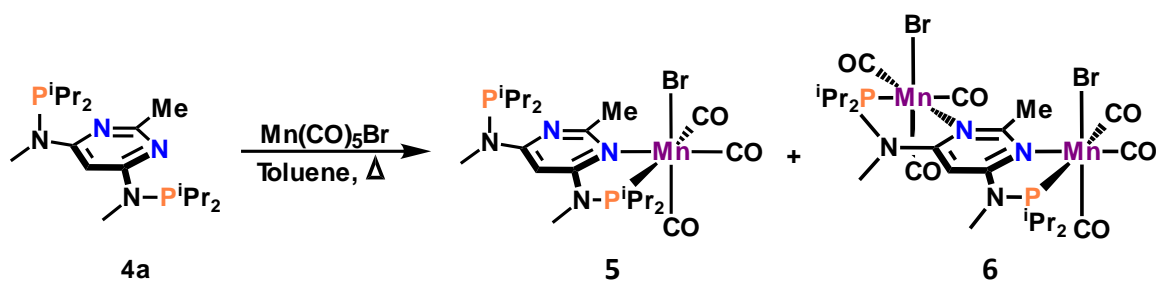
Scheme 14 Ligand synthesis

The synthesis route known from literature⁷⁰ was adapted at some critical steps. One of those steps was the twofold chlorination of the hydroxy-ketone compound. By redistillation of residual POCl₃, time-consuming quenching with ice and water followed by adjustment of the suspension to pH 7 with solid NaOH could be drastically accelerated.

Another adaption was the use of a copper(I) catalyst for amination with MeNH₂. Amination of electron-poor aryls was described by Buchwald⁷¹ and Hartwig⁷² using palladium catalysts. However, the catalyst employed was a Cu(I) salt and therefore a modification of the amination route for aryl halides reported by Buchwald and co-workers.⁷³ Upon addition of 5 mol-% of CuI amination of the dichloride compounds could be performed at 120°C without the need for microwave radiation.

3.2 Synthesis of Complexes

Synthesis of the mononuclear manganese(I) complex was conducted in toluene. Although the desired mononuclear product was obtained, analysis *via* ³¹P{¹H}-NMR spectra quickly revealed inherent difficulties.



Scheme 15 Formation of mono- and binuclear Mn(I) complexes

Unfortunately, a mixture of mono- and binuclear products was obtained upon attempts to synthesize $[\text{Mn}(\kappa^2\text{-}P,N\text{-methyl-pyrimidine})\text{Br}(\text{CO})_3]$ **5** (Scheme 15). Undesired formation of **6** could not be suppressed by variation of reaction conditions or precursor equivalents.

In $^{31}\text{P}\{^1\text{H}\}$ -NMR spectra (Figure 10) signals can be found at 143.1 ppm for the phosphorous coordinated to Mn(I) and 71.5 ppm for the phosphorous belonging to the free arm for the mononuclear complex $[\text{Mn}(\kappa^2\text{-}P,N\text{-methyl-pyrimidine})\text{Br}(\text{CO})_3]$ **5**. Both signals are shifted compared to the phosphorous signal of the free ligand at 69.4 ppm. In addition, IR spectra of the obtained product displayed characteristic carbonyl signals.

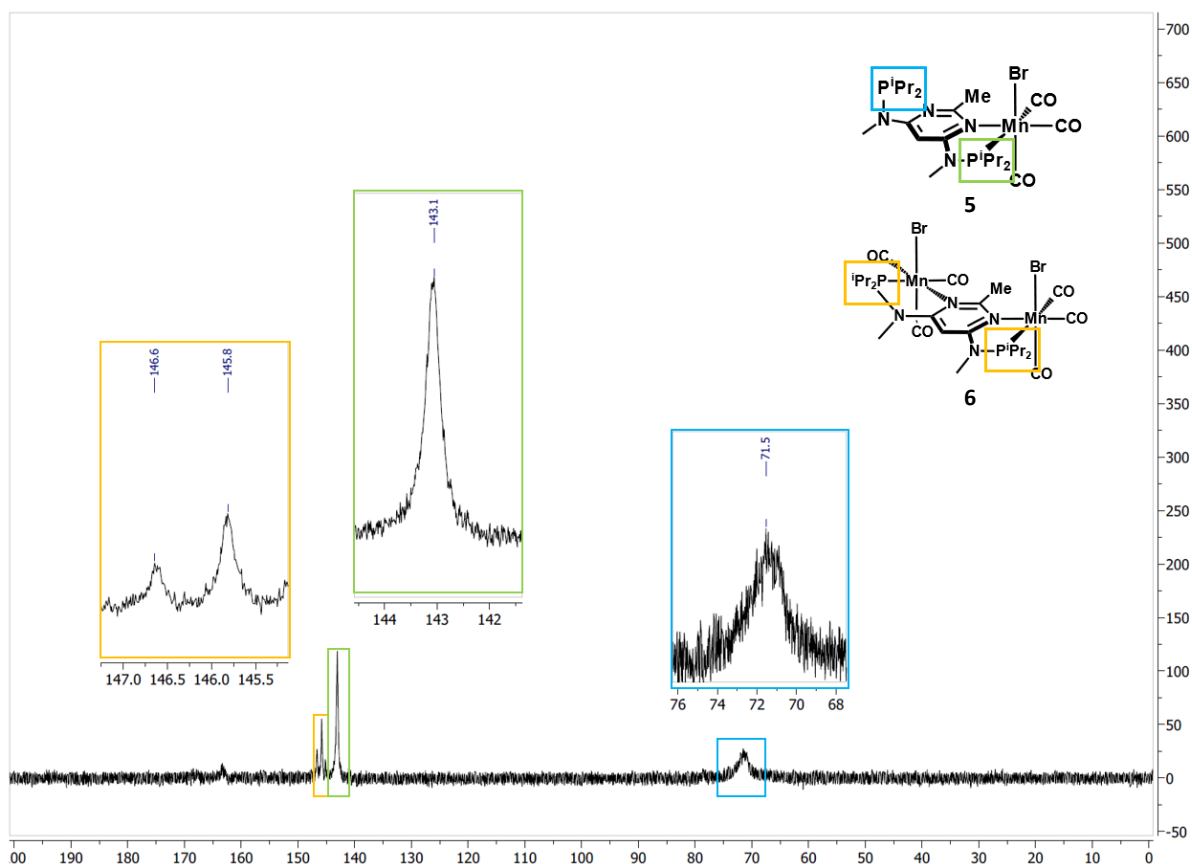


Figure 10 $^{31}\text{P}\{^1\text{H}\}$ NMR of the complexation of **4a** with $\text{Mn}(\text{CO})_5\text{Br}$

Two additional peaks appear noticeable in $^{31}\text{P}\{^1\text{H}\}$ NMR spectra (Figure 10) at 145.8 and 146.6 ppm. These signals belong to the two isomers of the binuclear complex $[\mu^2-(\kappa^2\text{-}P,N\text{-methyl-pyrimidine})\{\text{Mn}(\text{CO})_3\text{Br}\}_2]$ **6** (Figure 11). The two isomers **6a** and **6b** are formed in the ratio of approximately 2:1 which could be estimated from $^{31}\text{P}\{^1\text{H}\}$ NMR. Unfortunately, it could not be determined which isomer is formed preferentially.

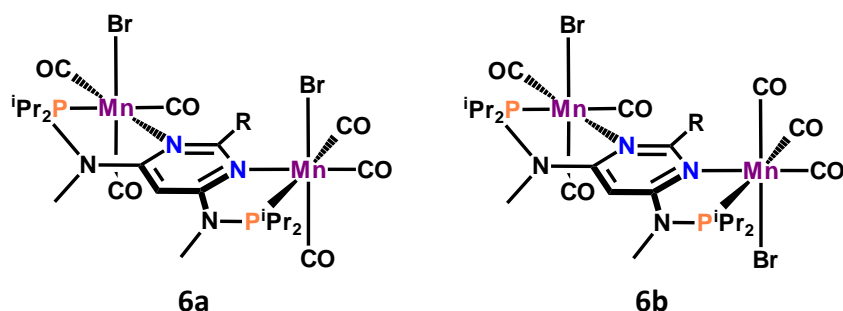
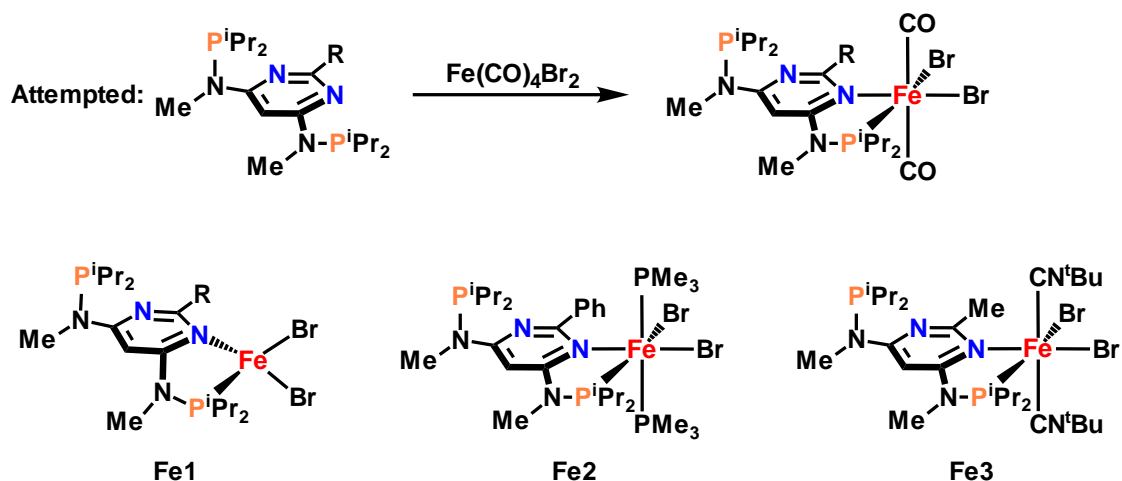


Figure 11 Isomers of $[\mu^2-(\kappa^2\text{-}P,N\text{-methyl-pyrimidine})\{\text{Mn}(\text{CO})_3\text{Br}\}_2]$ **6**

The mixture of mono- and binuclear products was later found to be separable by extraction. Nevertheless, pure mononuclear Mn(I) complex **5** could not be obtained in sufficient yields.

Therefore, saturation of one coordination site was considered a feasible route towards complexes containing only one manganese center. One synthetic route was based on $\text{Fe}(\text{CO})_4\text{Br}_2$ as a precursor (Scheme 16, top).

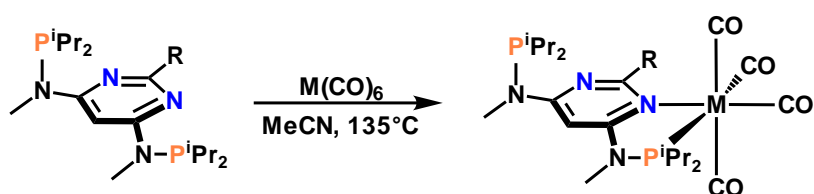


Scheme 16 Approach for the synthesis of Fe(II) complexes

Unfortunately the desired product could not be obtained, since first approaches resulted in the loss of all carbon monoxide ligands, monitored by IR spectroscopy. This adverse reaction most likely yielded the paramagnetic complex with tetrahedral geometry **Fe1** which could not be characterized *via* NMR analysis. Following routes were based upon either trapping or restoring the octahedral geometry using ligands with electronic properties similar to CO.

Efforts based on PMe_3 **Fe2** and $^t\text{BuNC}$ **Fe3** resulted in significant changes in color but later turned out to lead to decomposition of the complex.

Since coordination of group 6 metals had already been reported⁷⁴, saturation of one coordination site by chromium, molybdenum or tungsten was contemplated. The synthesis of complexes consisting of Me-Pyrim **4a** and Ph-Pyrim **4b** and group 6 transition metals (Scheme 17) was straightforward and afforded good yields under solvothermal conditions in MeCN. Removal of residual hexacarbonyl was sufficiently achieved by filtration through celite and yields up to 60 % could be obtained.



Scheme 17 Synthesis of mononuclear group 6 metal complexes

As supposed the use of 0.95 equivalents of hexacarbonyl resulted in the formation of mainly mononuclear complex, which was proved by $^{31}\text{P}\{^1\text{H}\}$ NMR analysis (Figure 12).

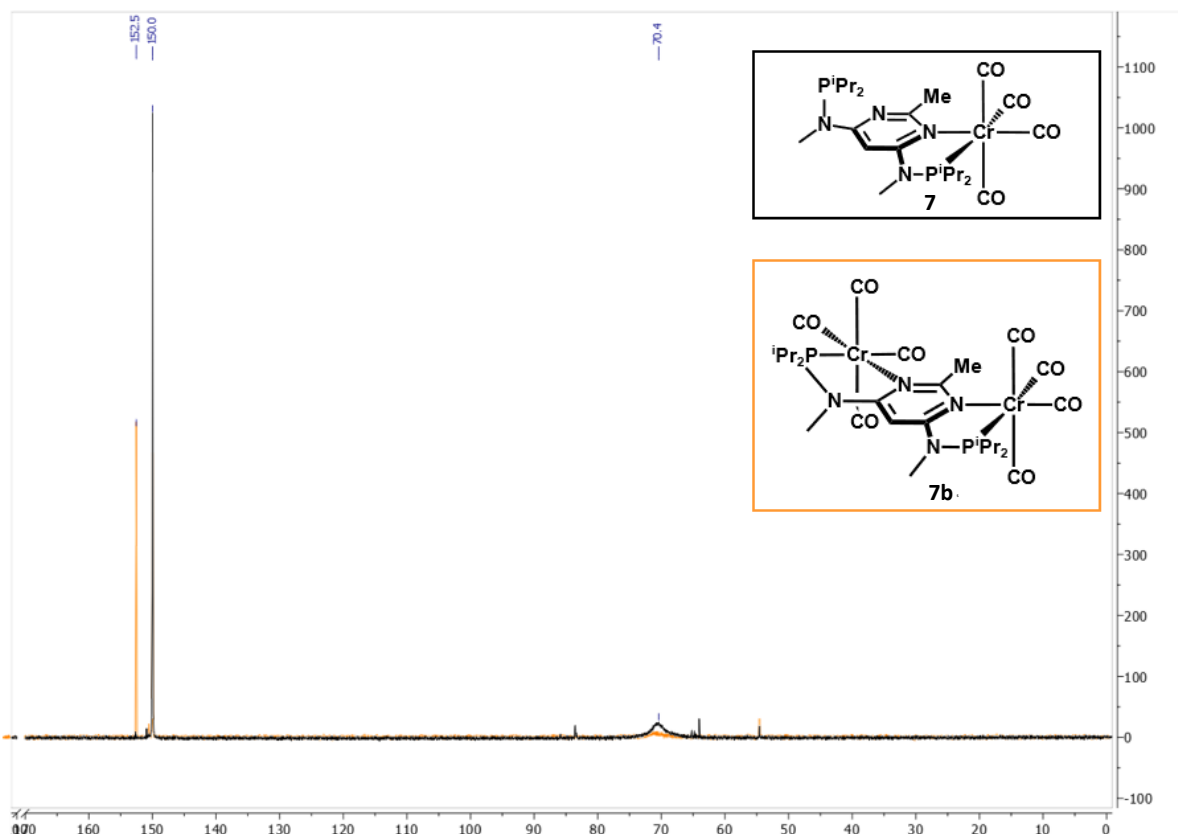


Figure 12 $^{31}\text{P}\{^1\text{H}\}$ NMR spectra of the complexation of Me-Pyrim **4a** with $\text{Cr}(\text{CO})_6$

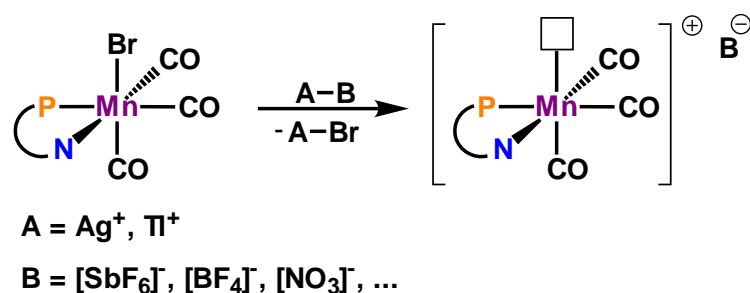
Two peaks can be found in the spectrum of $[\text{Cr}(\kappa^2\text{-}P,N\text{-methyl-pyrimidine})(\text{CO})_4]$ **7**: one at 150.3 ppm from the ligand site bearing the metal atom and another one at 70.4 ppm being the free arm of the ligand (Figure 12, black). If more than 0.95 equivalents of hexacarbonyl were applied, formation of the binuclear complex was observed. This could be detected *via* the signal at 152.5 ppm (Figure 12, orange).

3.3 Alkylation of Complexes

Alkylation of the Mn(I) center was supposed to give complexes capable of migratory insertion. Attempts of treating bidentate manganese complex **6** with sodium potassium alloy (Na/K) were made.⁵⁴ Since an anionic intermediate was supposed to be formed, subsequent alkylation was carried out with an organic halide e.g. bromopropane or iodomethane. However, instead of successfully yielding an alkylated compound the deployed conditions only led to decomposition of the complex. Similar results were obtained for the direct treatment of different bromide precursors with nucleophilic alkylation agents like methyllithium.

Therefore, another pathway was investigated as milder alternative for performing alkylation reactions. In advance, precursors were treated with halide abstraction reagents (Scheme 18). The formed cationic intermediate should then be transformed into the alkyls by treatment with organozinc reagents.

First approaches were based on the binuclear Mn(I) complex **6**. Unfortunately, removal of bromide by using $\text{Ag}[\text{SbF}_6]$ or $\text{Ag}[\text{BF}_4]$ to yield insoluble AgBr and the cationic complex with the non-coordinating counterion soon revealed drawbacks. Silver ions were hard to separate, which resulted in constant darkening of solutions even after numerous filtration steps. Therefore, $\text{Tl}[\text{BF}_4]$ was later employed as abstraction agent and showed to be separable much more easily *via* filtration.



Scheme 18 Halide abstraction

Unfortunately, $^{19}\text{F}\{^1\text{H}\}$ -NMR of the supposed product persistently showed fluorine signals. Hydrofluoric acid employed in the synthesis of $\text{Tl}[\text{BF}_4]$ was assumed to cause formation of thallium fluoride. Thus, substitution of the bromide ligand for fluoride seemed plausible and would have afforded a neutral complex. Due to good performance, TlNO_3 was chosen as available and inexpensive alternative.

Removal of the halide is a crucial step towards the alkylated complexes since the cationic complex is more reactive and therefore more easily accessible to the alkylating agent. One disadvantage to the abstraction route is the formation of a tetracarbonyl species.⁷⁵ Partial decomposition of the cationic species was assumed to release carbon monoxide, that occupies the vacant site. An indication to that was the appearance of a significant IR band together with the formation of a white solid that was insoluble in all common organic solvents. The IR band is shifted into a wave number range unusually high for CO bound to Mn(I) since it is found at 2107 cm^{-1} (Figure 13).

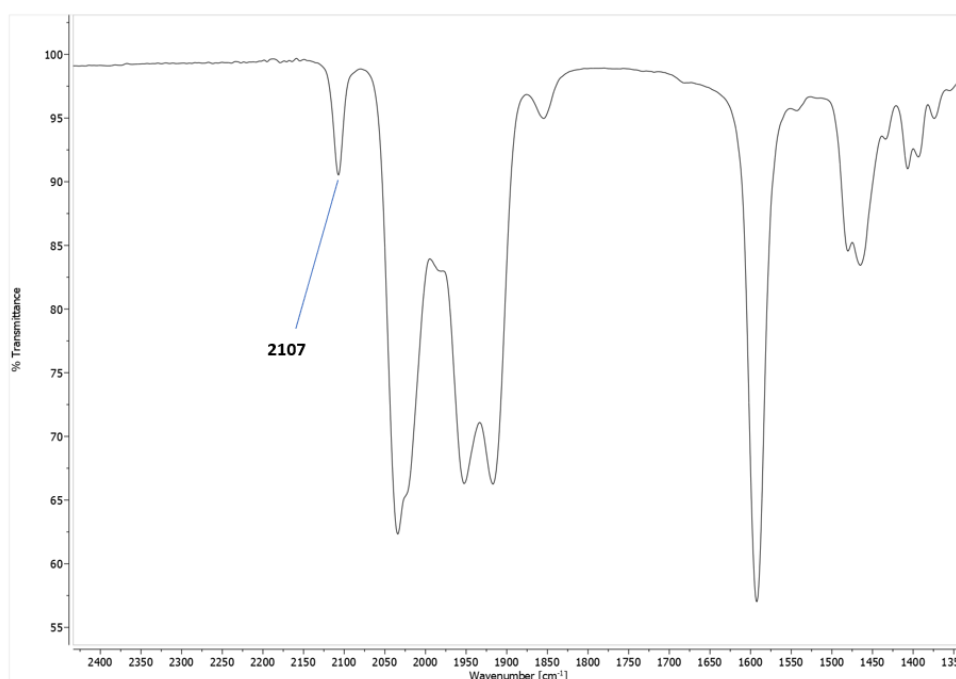


Figure 13 IR spectra of **6** treated with 2 equiv of $\text{Tl}[\text{BF}_4]$

Later on, precursor **6** was replaced by the binuclear complexes **13**, **14** and **15** containing group 6 metals centers. This was based on the realization that assessment of $^{31}\text{P}\{^1\text{H}\}$ -NMR spectra was complicated by the occurrence of the two isomers **6a** and **6b**. Heterobinuclear complexes were chosen as precursors, since the corresponding $^{31}\text{P}\{^1\text{H}\}$ -NMR spectra contained a sharp

and recognizable peak as reference. Moreover, these complexes were obtained in higher yields and purity in comparison to **6**.

Substitution of precursors entailed an exchange of the alkylating agent as well. Organolithium compounds like MeLi are too reactive and could possibly attack the carbon atoms of the carbon monoxide ligands coordinated to the group 6 metals. Therefore, less reactive organozinc compounds were chosen as a suitable alternative. As a last correction of reaction conditions previously investigated, the solvent was replaced by THF.

IR spectroscopy was considered to be a convenient way of monitoring the performed reactions. The obtained spectra seemed plausible, since the characteristic band belonging to CO in the position *trans* to bromide showed comprehensible changes in wave number. Unfortunately, it later turned out that some sample discrimination must have occurred. Although the $^{31}\text{P}\{^1\text{H}\}$ -NMR spectra showed various peaks, the IR spectra displayed only the desired tricarbonyl bands and therefore led to the conclusion that one clean product was obtained.

$^{31}\text{P}\{^1\text{H}\}$ -NMR spectra of the complexes treated with a halide abstraction agent suggested partial decomposition. Since this indicated an unstable cationic intermediate, presence of a nucleophilic carbon atom should contain this adverse reaction. Therefore, TINO_3 and the organozinc compound were added simultaneously. These one-pot reactions were monitored *via* NMR.

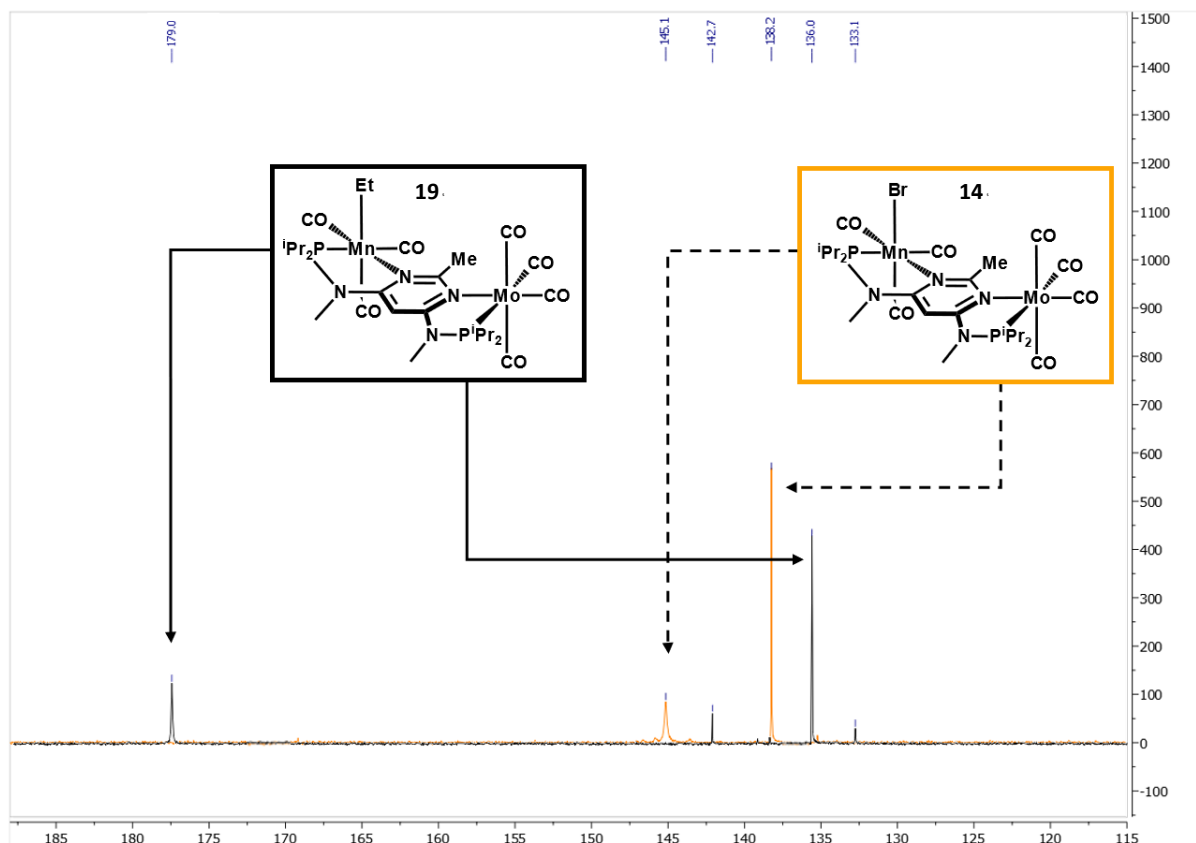


Figure 14 $^{31}\text{P}\{^1\text{H}\}$ -NMR spectra of the reaction of **14** with TINO_3 and Et_2Zn

$^{31}\text{P}\{^1\text{H}\}$ -NMR spectra of the reaction of complex **14** with TINO_3 and Et_2Zn (Figure 14) shows a new signal at 179.0 ppm, probably belonging to the phosphorous coordinated to manganese now bearing an ethyl ligand. The signal of the phosphorous coordinated to molybdenum is shifted to 136.0 ppm. Signals at 142.7 and 133.1 ppm can be identified as signals from the starting material by comparison with $^{31}\text{P}\{^1\text{H}\}$ -NMR of **14**. Shifts of the starting material peaks are caused by changing the NMR solvent to $\text{THF-}d_8$.

To verify the origin of the signal at 179.0 ppm a ^{31}P - ^1H -HMBC spectra was recorded (Figure 15). Crosspeaks with protons of the ligand system with shifts above 1.00 ppm can be found for both phosphorous signals at 136.0 and 179.0 ppm. However, one crosspeak arises from the correlation of a phosphorous donor with a hydrogen atom at 0.20 ppm. Since this shift range is common for alkyl groups coordinated to Mn(I), it indicates successful alkylation of the complex.⁵⁴ Thus, the signal at 179.0 ppm showing this correlation was assigned to the phosphorous atom coordinated to manganese.

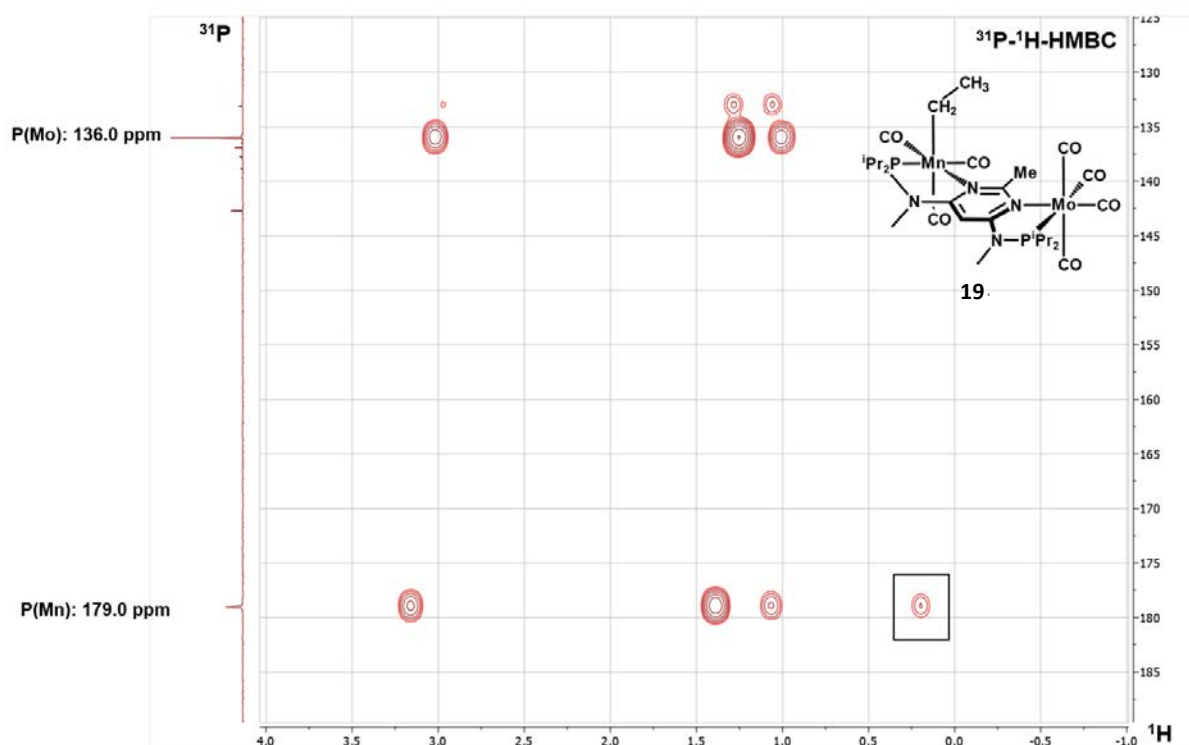


Figure 15 ^{31}P - ^1H -HMBC of the reaction of **14** with TiNO_3 and Et_2Zn

Similar results were found for the reaction between **14** and Me_2Zn . The recorded $^{31}\text{P}\{^1\text{H}\}$ NMR spectra (Figure 16) shows shifted signal of the phosphorous coordinated to the presumably methylated Manganese at 157.6 ppm.

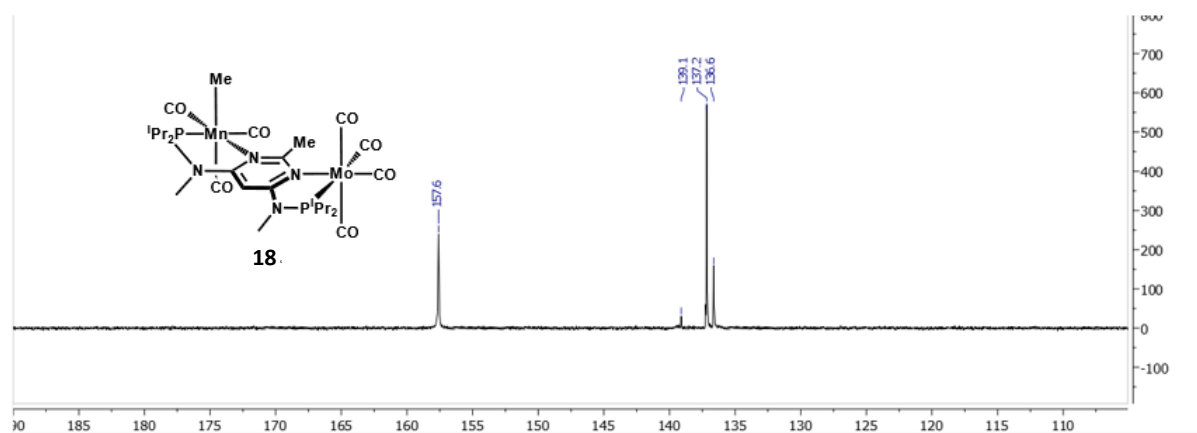


Figure 16 $^{31}\text{P}\{^1\text{H}\}$ -NMR spectra of the reaction of **13** with TiNO_3 and Me_2Zn

The corresponding HMBC spectra (Figure 17) shows a crosspeak of the significantly shifted phosphorous atom at 157.6 ppm with a proton signal shifted far-off the known ligand signals to -1.02 ppm.



Figure 17 $^{31}\text{P}\text{-}^1\text{H}\text{-HMBC}$ of the reaction of **14** with TINO_3 and Me_2Zn

Binuclear complex **15** containing tungsten and manganese was treated with TINO_3 and an organozinc compound. $^{31}\text{P}\{^1\text{H}\}$ -NMR spectra (Figure 18) bear a striking resemblance to those obtained for molybdenum complexes **18** and **19**. The reaction with Me_2Zn led to a peak at 157.8 ppm in $^{31}\text{P}\{^1\text{H}\}$ -NMR spectra. Upon treatment of **15** with Et_2Zn a signal was detected at 179.7 ppm.

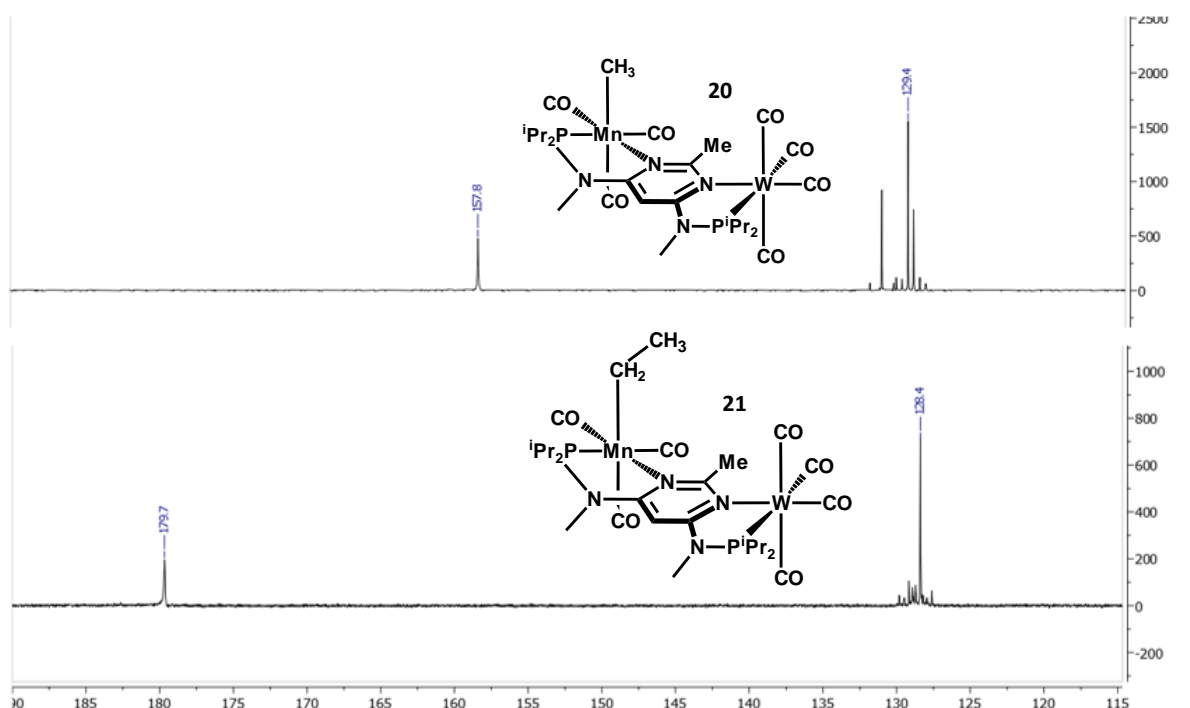


Figure 18 $^{31}\text{P}\{^1\text{H}\}$ -NMR spectra of the reaction of **15** with TINO_3 and Me_2Zn (top) or Et_2Zn (bottom)

Attempts to isolate the alkylated species were made. Unfortunately, no satisfying results could be obtained so far. Therefore, different protocols for quenching the residual diorganozinc compound and isolation of the alkylated products are currently under investigation.

4 Conclusion and Outlook

Within this work, PN-based binuclear complexes bearing a manganese(I) center were synthesized.

Synthesis of the pyrimidine PN-ligand was straightforward. Modifications involved the redistillation of POCl_3 and the use of a Buchwald-Hartwig type amination procedure.

Since the mononuclear manganese complex could not be synthesized in acceptable yields, saturation of the second coordination site with chromium, molybdenum or tungsten was required.

First alkylation approaches utilizing sodium potassium alloy (Na/K) or direct treatment with nucleophilic alkylation reagents led to decomposition of the complexes. An alternative pathway was studied involving halide abstraction and diorganozinc compounds as milder alkylation agents. Simultaneous treatment of the bromide precursors with TINO_3 and R_2Zn in THF turned out to be the most suitable reactions conditions and NMR spectra indicate successful alkylation.

So far, alkylated complexes were based on the Me-Pyrim ligand within this thesis. Investigation of complexes based on the Ph-Pyrim ligand would be of interest, since this change of the pyrimidine moiety could significantly tailor the stereo-electronic properties of the whole system. Furthermore, related systems bearing a chromium metal center may be interesting. Modifications to the alkylation protocol might be required for this type of complexes.

Strategies for isolation of the alkylated complexes are currently under investigation. Studies on behavior and catalytic reactivity of the isolated species will subsequently be of great interest.

5 Experimental Part

5.1 Materials and Methods

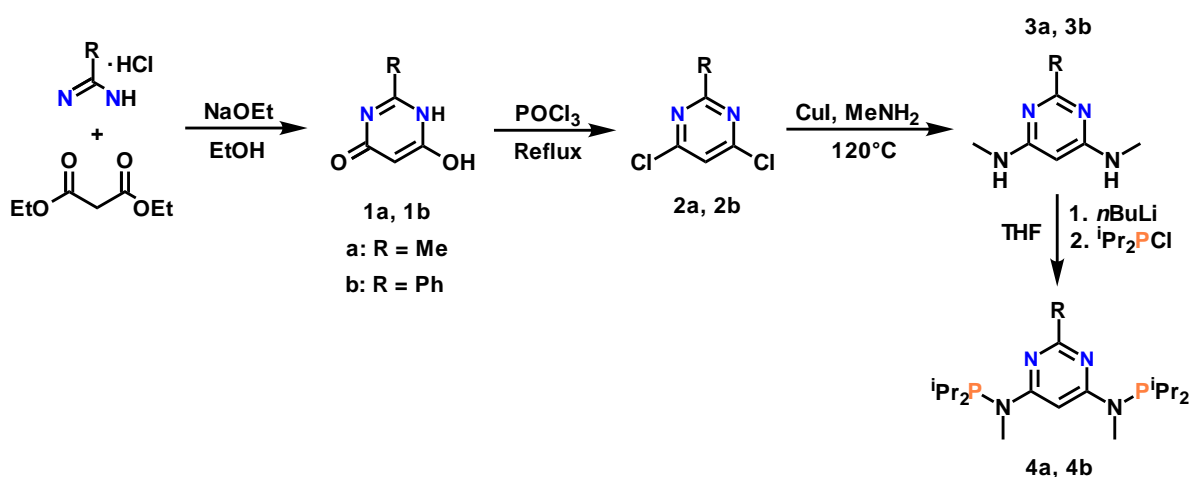
All manipulations were performed under inert conditions by using Schlenk techniques or in a MBraun inert-gas glovebox. Dry solvents were purified according to standard procedures. Deuterated solvents were purchased from Aldrich and dried over 3 Å molecular sieves. All starting materials are known compounds and were used as obtained from commercial sources.

^1H , $^{13}\text{C}\{^1\text{H}\}$, and $^{31}\text{P}\{^1\text{H}\}$ NMR spectra were recorded on Bruker AVANCE-400 and AVANCE-600 spectrometers. ^1H and $^{13}\text{C}\{^1\text{H}\}$ NMR spectra were referenced internally to residual protic solvent and solvent resonances are reported relative to tetramethylsilane ($\delta = 0$ ppm). $^{31}\text{P}\{^1\text{H}\}$ NMR spectra were referenced externally to H_3PO_4 (85 %) ($\delta = 0$ ppm).

GC-MS analysis was conducted on an ISQ LT Single quadrupole MS (Thermo Fisher) directly interfaced to a TRACE 1300 Gas Chromatographic System (Thermo Fisher), using a Rxi-5Sil MS (30 m, 0.25 mm ID) cross-bonded dimethyl Polysiloxane capillary column at a carrier flow of He (1.5 mL/min).

5.2 Synthesis of Ligands

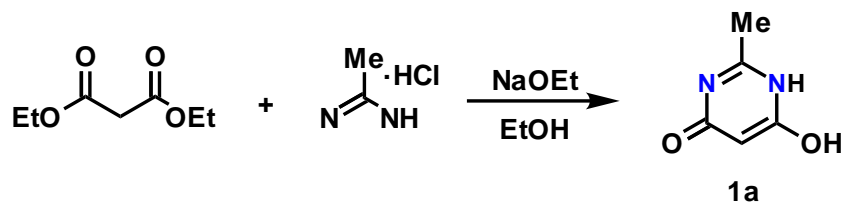
Two pyrimidine-based ligands were synthesized according to literature (Scheme 19).⁷⁰



Scheme 19 Ligand synthesis

5.2.1 Synthesis of *N4,N6*-Bis(diisopropylphosphino)-*N4,N6,2*-trimethylpyrimidine-4,6-diamine (Me-Pyrim)

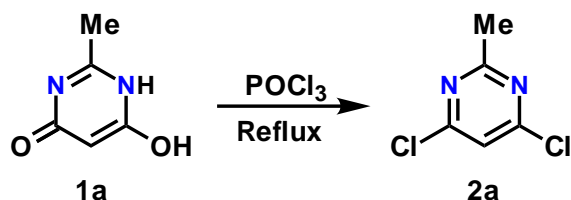
6-Hydroxy-2-methylpyrimidin-4(1H)-one (1a)



In a 250 mL three-necked flask sodium (7 g, 304 mmol, 3.0 equiv) was dissolved in ethanol (130 mL) overnight. Acetamidine hydrochloride (10.23 g, 108 mmol, 1.1 equiv) and diethylmalonate (15 mL, 98 mmol, 1.0 equiv) were added and the resulting white suspension was refluxed for 3 hours. It was cooled to 0°C and the pH was adjusted to 2 using hydrochloric acid (37 %, 15 mL). The resulting precipitate was filtered, washed with cold water (3 x 100 mL) and dried under vacuum. **1a** was obtained as a white solid (9.87 g, 80 %).

¹H NMR (400 MHz, DMSO, 25°C): δ = 4.98 (s, 1H, Pyrim-H), 3.36 (br, 2H, OH), 2.24 (s, 3H, CH₃) ppm.

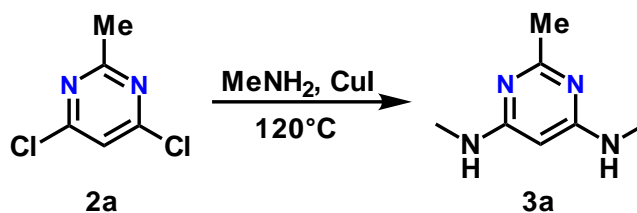
4,6-Dichloro-2-methyl-pyrimidine (2a)



1a (3.8 g, 30 mmol, 1 equiv) and POCl₃ (58 mL, 624 mmol, 20.7 equiv) were placed in a 100 mL round-bottom flask and refluxed overnight. After cooling to room temperature the flask was equipped with a distillation bridge and most of excess POCl₃ was removed. Ice was added to the resulting brown liquid and the solution was adjusted to neutral pH using solid NaOH. After filtration and washing with cold water **2a** was obtained as a crystalline, brown solid (2.4 g, 49 %).

¹H NMR (400 MHz, DMSO, 25 °C): δ = 7.87 (s, 1H, Pyrim-H), 2.61 (s, 3H, CH₃) ppm.

***N*4,*N*6,2-Trimethylpyrimidine-4,6-diamine (**3a**)**

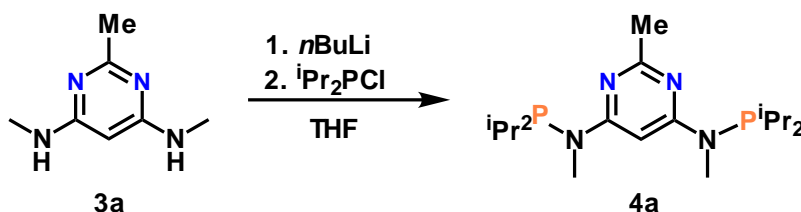


In a sealed microwave glass vial **2a** (1 g, 6 mmol, 1 equiv) was heated with CuI (0.06 g, 0.3 mmol, 0.05 equiv) and MeNH₂ (40% in water, 5 mL) to 120°C overnight. The suspension was filtrated, washed with cold water (3 x 10 mL) and dried under vacuum to yield a white solid (0.8 g, 86 %).

¹H NMR (400 MHz, DMSO, 25°C): δ = 5.07 (s, 1H, Pyrim-H), 2.68 (d, J = 4.9 Hz, 6H, N-CH₃), 2.14 (s, 3H, CH₃) ppm.

RT (GC): 5.63 min MS: 152.09 m/z [M⁺]

***N*4,*N*6-Bis(diisopropylphosphino)-*N*4,*N*6,2-trimethylpyrimidine-4,6-diamine (**4a**)**



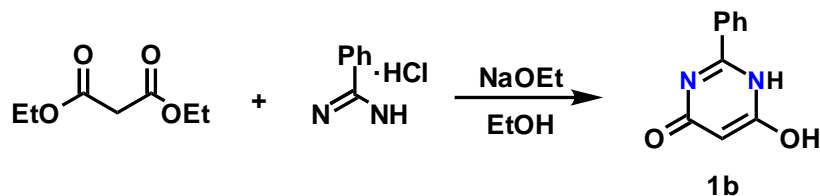
In a three-necked flask a suspension of **3a** (2.0 g, 13 mmol, 1.0 equiv) in THF (40 mL) was cooled to -90°C and *n*BuLi (1.6 M in hexane, 17 mL, 28 mmol, 2.1 equiv) was added slowly. After completed addition the suspension was kept at -90°C for another 15 minutes. It was then allowed to warm up to room temperature and was stirred for 3 hours before addition of *i*Pr₂PCl (4.4 mL, 28 mmol, 2.1 equiv). After stirring overnight the volume of the solution was reduced to a third and the resulting suspension was extracted with toluene (4 x 30 mL). **4a** was obtained as a white waxy solid (3.01 g, 60 %) by recrystallization from methanol (2 mL).

¹H NMR (400 MHz, CD₂Cl₂, 25°C): δ = 6.94 (s, 1H, Pyrim-H), 2.93 (d, J = 2.2 Hz, 6H, N-CH₃), 2.25 (s, 3H, Me), 2.12 (br, 4H, CH(CH₃)₂), 1.14 – 0.80 (m, 23H, CH(CH₃)₂) ppm.

³¹P{¹H} NMR (162 MHz, CD₂Cl₂, 25°C): δ = 69.4.

5.2.2 Synthesis of *N*4,*N*6-bis(diisopropylphosphino)-*N*4,*N*6-dimethyl-2-phenylpyrimidine-4,6-diamine (Ph-Pyrim)

6-Hydroxy-2-phenylpyrimidin-4(1H)-one (1b)

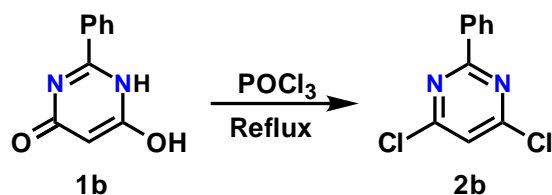


In a 250 mL three-necked flask sodium (7 g, 304 mmol, 3.0 equiv) was dissolved in 130 mL of ethanol overnight. Benzamidine hydrochloride (10.16 g, 65 mmol, 1.1 equiv) and diethylmalonate (9 mL, 59 mmol, 1.0 equiv) were added and the resulting white suspension was refluxed for 4 hours. It was cooled to 0°C and the pH was adjusted to 2 using hydrochloric acid (37 %, 10 mL). The resulting precipitate was filtered, washed with cold water (3 x 100 mL) and dried under vacuum. The product was obtained as a slightly beige solid (5.50 g, 50 %).

¹H NMR (400 MHz, CDCl₃, 25°C): δ = 12.89 (s, 1H, OH), 8.41 – 8.33 (m, 2H, Ph), 8.15 (m, 1H, Ph), 7.59 – 7.38 (m, 2H, Ph), 6.45 (s, 1H, Pyrim-H) ppm.

RT (GC): 6.20 min 188.97 m/z [M⁺]

4,6-Dichloro-2-phenylpyrimidine (2b)

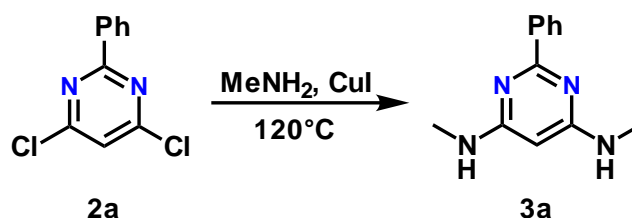


6-Hydroxy-2-phenylpyrimidin-4(1H)-one **1b** (2.5 g, 13 mmol, 1 equiv) and POCl₃ (60 mL, 646 mmol, 48,6 equiv) were placed in a 100 mL round-bottom flask and refluxed overnight. After cooling to room temperature the flask was equipped with a distillation bridge and most of excess POCl₃ was removed. Ice was added to the resulting brown liquid and the solution was adjusted to neutral pH using solid NaOH. After filtration and washing with cold water (40 mL) the product was obtained as a white solid (2.1 g, 70 %).

^1H NMR (400 MHz, DMSO, 25°C): δ = 8.16 – 8.00 (m, 2H, Ph), 7.64 – 7.39 (m, 3H, Ph), 5.39 (s, 1H, Pyrim-H) ppm.

RT (GC): 6.20 min 223.93 m/z [M^+]

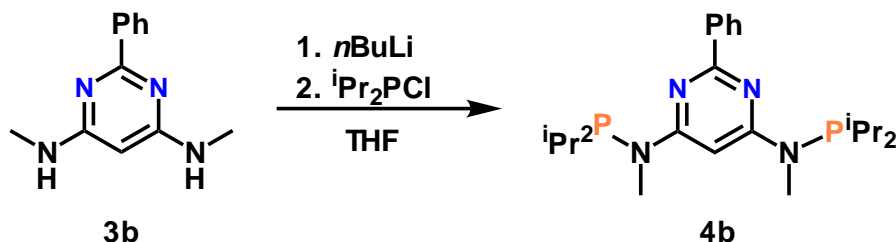
***N*4,*N*6-Dimethyl-2-phenylpyrimidine-4,6-diamine (**3b**)**



In a sealed microwave glass vial 4,6-Dichloro-2-phenylpyrimidine **2b** (1 g, 4 mmol, 1 equiv) was heated with CuI (0.04 g, 0.4 mmol, 0.05 equiv) and MeNH_2 (40% in water, 5 mL) to 120°C overnight. The suspension was filtrated, washed with cold water (4 x 10 mL) and dried under vacuum to yield a beige solid (1.74 g, 91 %).

^1H NMR (400 MHz, DMSO, 25°C): δ = 8.36 – 8.27 (m, 2H, Ph), 7.48 – 7.37 (m, 3H, Ph), 6.57 (m, J = 4.9 Hz, 2H, NH), 5.27 (s, 1H, Pyrim-H), 2.81 (d, J = 4.9 Hz, 6H, N- CH_3) ppm.

***N*4,*N*6-Bis(diisopropylphosphino)-*N*4,*N*6-dimethyl-2-phenylpyrimidine-4,6-diamine (**4b**)**



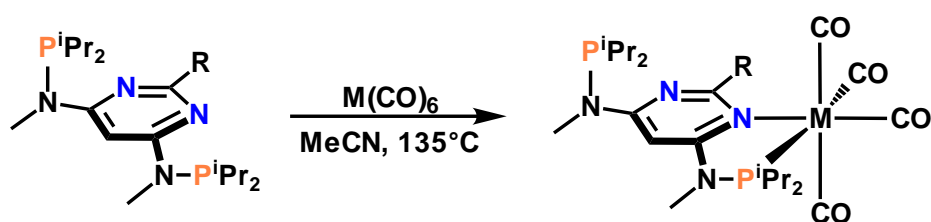
In a three-necked flask a solution of **3b** (1.74 g, 8 mmol, 1.0 equiv) in THF (40 mL) was cooled to -90°C and $n\text{BuLi}$ (1.6 M in hexane, 11 mL, 17 mmol, 2.1 equiv) was added slowly. After completed addition the suspension was kept at -90°C for another 15 minutes. It was then allowed to warm up to room temperature and was stirred for 3 hours before addition of $i\text{Pr}_2\text{P-Cl}$ (2.6 mL, 17 mmol, 2.1 equiv). After stirring overnight the solvent was removed under vacuum and the resulting solid was extracted with toluene (4 x 10 mL) and filtrated through silica. **4b** was obtained as a white solid (3.30 g, 91 %).

^1H NMR (400 MHz, CD_2Cl_2 , 25°C): δ = 8.47 – 8.39 (m, 2H, Ph), 7.48 – 7.38 (m, 3H, Ph), 7.25 – 7.02 (m, 1H, Pyrim-H), 3.17 (d, J = 2.6 Hz, 6H, N- CH_3), 2.33 (d, J = 16.4 Hz, 4H, $\text{CH}(\text{CH}_3)_2$), 1.39 – 0.85 (m, 24H, $\text{CH}(\text{CH}_3)_2$) ppm.

$^{31}\text{P}\{^1\text{H}\}$ NMR (162 MHz, CD_2Cl_2 , 25°C): δ = 68.3 ppm.

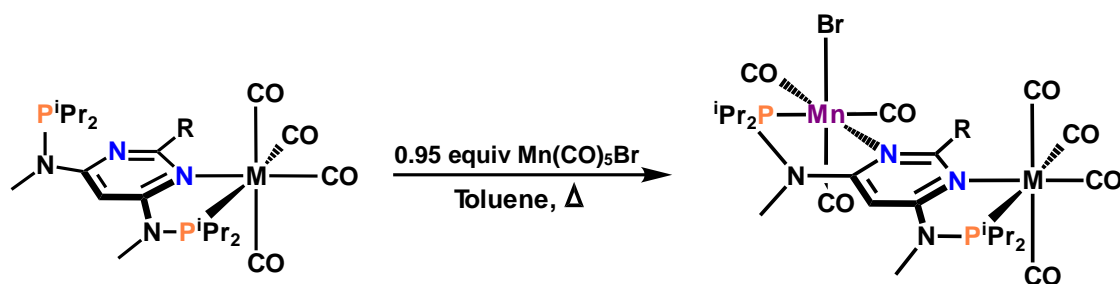
5.3 Synthesis of Complexes

Mononuclear complexes consisting of chromium, molybdenum or tungsten centers were synthesized according to literature (Scheme 20).⁷⁴



Scheme 20 Mononuclear group 6 metal complex synthesis

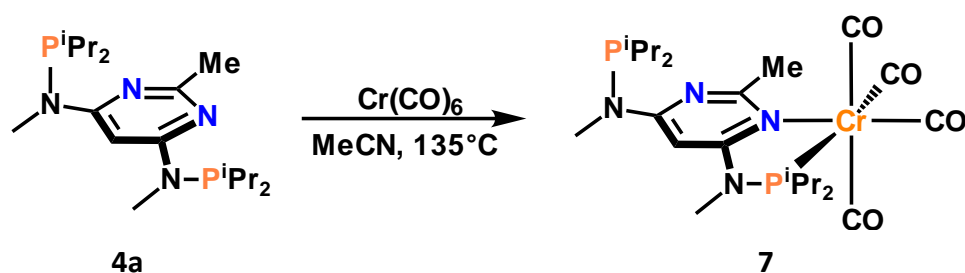
For the synthesis of the binuclear complexes as well as for the mononuclear Manganese complex, implementation of manganese(I) was performed using a different solvent and lower temperatures. Linkage to the free ligand yielded the mono- or homobinuclear Mn(I) complex. Reaction with the mononuclear group 6 complexes led to the formation of the heterobinuclear complexes (Scheme 21).



Scheme 21 Synthesis of binuclear complexes

5.3.1 Synthesis of Mononuclear Complexes

[Cr(κ^2 -*P,N*-methyl-pyrimidine)(CO)₄] (7)



In a microwave glass vial Cr(CO)₆ (0.109 g, 0.49 mmol, 0.95 equiv) was added to a solution of **4a** (0.200 g, 0.52 mmol, 1 equiv) in MeCN (2 mL). The vial was sealed and heated to 135°C overnight. The resulting yellow solution was allowed to cool and was filtrated through celite. Yellow solid that formed upon cooling was dissolved in DCM (2 mL) and filtrated through celite. The solvent was removed under vacuum to yield a yellow solid (0.168 g, 62 %).

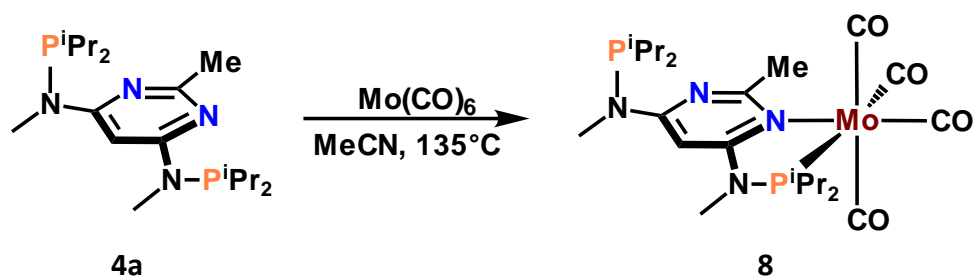
¹H NMR (600 MHz, CD₂Cl₂, 25°C): δ = 6.42 (s, 1H, Pyrim-H), 3.02 (d, J = 1.5 Hz, 3H, N-CH₃), 2.94 (d, J = 3.0 Hz, 3H, N-CH₃), 2.82 (s, 3H, Me), 2.63 – 2.51 (m, 2H, CH(CH₃)₂), 2.17 (s, 2H, CH(CH₃)₂), 1.45 – 0.93 (m, 24H, CH(CH₃)₂) ppm.

¹³C{¹H} NMR (151 MHz, CD₂Cl₂, 25°C): δ = 229.3 (d, J = 14.2 Hz, CO), 226.4 (d, J = 3.0 Hz, CO), 220.9 (d, J = 14.2 Hz, CO), 170.1 (Pyrim-C²), 167.7 – 167.4 (m, Pyrim-C^{4/6}), 167.2 (d, J = 22.8 Hz, Pyrim-C^{4/6}), 85.2 (d, J = 30.7 Hz, Pyrim-C⁵), 33.7 (d, J = 6.4 Hz, N-CH₃), 32.5 - 32.2 (s/s/s, N-CH₃, Pyrim-CH₃, CH(CH₃)₂), 26.7 – 26.2 (m, CH(CH₃)₂), 19.99 – 18.30 (m, CH(CH₃)₂) ppm.

³¹P{¹H} NMR (243 MHz, CD₂Cl₂, 25°C): δ = 149.9, 70.5 ppm.

IR (ATR, cm⁻¹): 2001 (ν_{CO}), 1872 (ν_{CO}), 1834 (ν_{CO}).

[Mo(κ^2 -*P,N*-methyl-pyrimidine)(CO)₄] (8)



In a microwave glass vial Mo(CO)₆ (0.130 g, 0.49 mmol, 0.95 equiv) was added to a solution of **4a** (0.200 g, 0.52 mmol, 1 equiv) in MeCN (2 mL). The vial was sealed and heated to 135°C overnight. The resulting yellow solution was allowed to cool and was filtrated through celite.

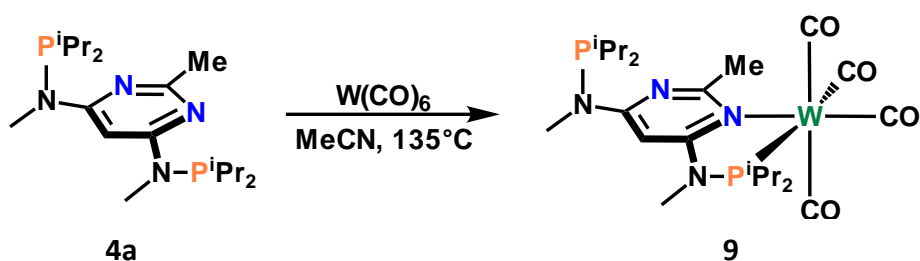
The solvent was evaporated under vacuum and the resulting solid was washed with *n*-pentane (2 x 7 mL) to yield a yellow powder (0.123 g, 42 %).

^1H NMR (400 MHz, CD_2Cl_2 , 25°C): δ = 6.47 (s, 1H, Pyrim-H), 3.04 (d, J = 1.5 Hz, 3H, N-CH₃), 2.95 (d, J = 3.1 Hz, 3H, N-CH₃), 2.78 (s, 3H, Me), 2.46 (m, 2H, $\underline{\text{C}}\text{H}(\text{CH}_3)_2$), 2.18 (m, 2H, $\underline{\text{C}}\text{H}(\text{CH}_3)_2$), 1.40 – 0.92 (m, 24H, $\text{CH}(\underline{\text{C}}\text{H}_3)_2$) ppm.

$^{31}\text{P}\{^1\text{H}\}$ NMR (162 MHz, CD_2Cl_2 , 25°C): δ = 134.0, 70.6 ppm.

IR (ATR, cm^{-1}): 2010 (ν_{CO}), 1875 (ν_{CO}), 1835 (ν_{CO}).

[W(κ^2 -*P,N*-methyl-pyrimidine)(CO)₄] (9)



In a microwave glass vial W(CO)_6 (0.087 g, 0.25 mmol, 0.95 equiv) was added to a solution of **4a** (0.100 g, 0.26 mmol, 1 equiv) in MeCN (2 mL). The vial was sealed and heated to 135°C overnight. The resulting yellowish brown solution was allowed to cool and was filtrated through celite. The solvent was evaporated under vacuum to yield a yellow solid (0.101 g, 60 %).

^1H NMR (400 MHz, CD_2Cl_2 , 25°C): δ = 6.50 (s, 1H, Pyrim-H), 3.05 (d, J = 1.4 Hz, 3H, N-CH₃), 2.96 (d, J = 3.3 Hz, 3H, N-CH₃), 2.84 (s, 3H, Me), 2.54 – 2.38 (m, 2H, $\underline{\text{C}}\text{H}(\text{CH}_3)_2$), 2.25 – 2.13 (m, 2H, $\underline{\text{C}}\text{H}(\text{CH}_3)_2$), 1.42 – 0.93 (m, 24H, $\text{CH}(\underline{\text{C}}\text{H}_3)_2$) ppm.

$^{31}\text{P}\{^1\text{H}\}$ NMR (162 MHz, CD_2Cl_2 , 25°C): δ = 126.1 (t, J = 124.7 Hz), 71.3 ppm.

IR (ATR, cm^{-1}): 2005 (ν_{CO}), 1866 (ν_{CO}), 1832 (ν_{CO}).

[Mn(κ^2 -*P,N*-methyl-pyrimidine)Br(CO)₃] (5)



In a Schlenk flask Mn(CO)₅Br (0.068 g, 0.25 mmol, 0.95 equiv) was added to a solution of N4,N6- **4a** (0.100 g, 0.26 mmol, 1 equiv) in toluene (5 mL). Upon heating to reflux the solution turned orange and CO gas emission was observed. The mixture was refluxed for ten minutes until no further gas emission occurred. The solvent was removed under vacuum and the resulting foam was washed with *n*-pentane (2 x 6 mL) to yield a yellow solid (0.067 g, 45 %).

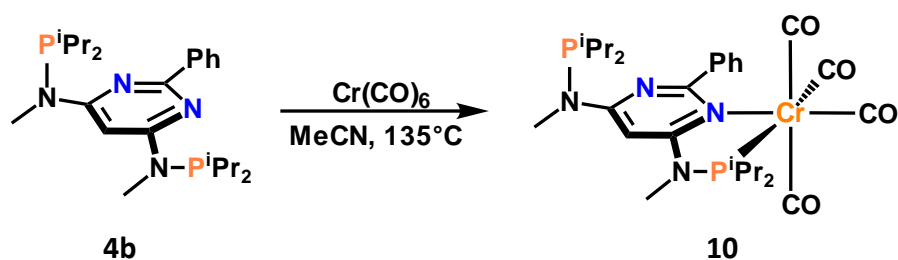
¹H NMR (600 MHz, CD₂Cl₂, 25°C): δ = 6.55 (s, 1H, Pyrim), 3.05 (s, 6H, N-CH₃), 3.01 (s, 3H, Me), 2.93 – 2.84 (m, 2H, CH(CH₃)₂), 2.83 – 2.74 (m, 2H, CH(CH₃)₂), 1.58 – 0.93 (m, 24H, CH(CH₃)₂) ppm.

¹³C{¹H} NMR (151 MHz, CD₂Cl₂, 25°C): δ = 223.4 (CO), 215.7 (CO), 169.4 (Pyrim-C²), 167.1 (Pyrim-C^{4/6}), 86.0 (Pyrim-C⁵), 37.27 (Me), 34.51 (d, *J* = 6.6 Hz, N-CH₃), 32.01 (d, *J* = 18.3 Hz, CH(CH₃)₂), 29.8 (d, *J* = 21.4 Hz, CH(CH₃)₂), 27.12 – 17.31 (m, CH(CH₃)₂).

³¹P{¹H} NMR (162 MHz, CD₂Cl₂, 25°C): δ = 143.1, 70.9 ppm.

IR (ATR, cm⁻¹): 2019 (ν_{CO}), 1934 (ν_{CO}), 1907 (ν_{CO}).

[Cr(κ^2 -*P,N*-phenyl-pyrimidine)(CO)₄] (10)



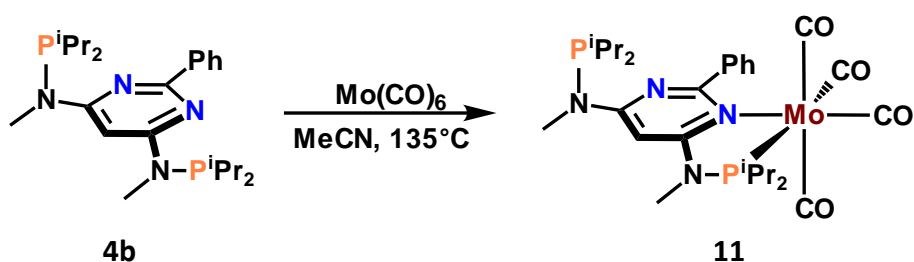
In a microwave glass vial Cr(CO)₆ (0.94 g, 0.43 mmol, 0.95 equiv) was added to a solution of **4b** (0.200 g, 0.45 mmol, 1 equiv) in MeCN (2 mL). The vial was sealed and heated to 135°C overnight. The resulting orange solution was allowed to cool and was filtrated through celite. The solvent was evaporated under vacuum and the residue was washed with *n*-pentane (3 mL) to yield a yellow solid (0.112 g, 43 %).

^1H NMR (400 MHz, CD_2Cl_2 , 25°C): $\delta = 7.71 - 7.32$ (m, 5H, Ph), 6.58 (s, 1H, Pyrim-H), 3.05 – 3.01 (m, 6H, N- CH_3), 2.69 – 2.52 (m, 2H, $\text{CH}(\text{CH}_3)_2$), 2.22 – 2.11 (m, 2H, $\text{CH}(\text{CH}_3)_2$), 1.45 – 0.86 (m, 24H, $\text{CH}(\text{CH}_3)_2$) ppm.

$^{31}\text{P}\{^1\text{H}\}$ NMR (162 MHz, CD_2Cl_2): $\delta = 148.17, 71.98$ ppm.

IR (ATR, cm^{-1}): 2002 (ν_{CO}), 1864 (ν_{CO}), 1835 (ν_{CO}).

[Mo(κ^2 -*P,N*-phenyl-pyrimidine)(CO) $_4$] (**11**)



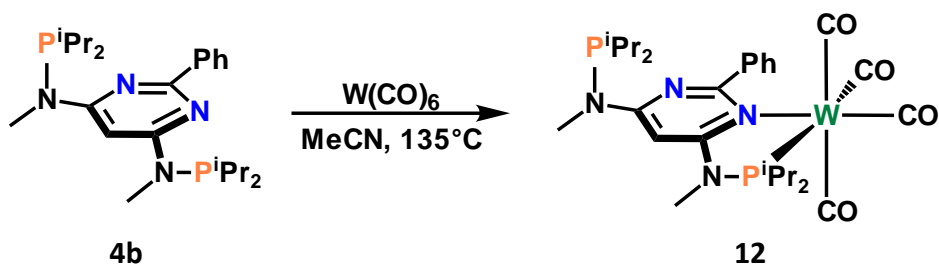
In a microwave glass vial $\text{Mo}(\text{CO})_6$ (0.056 g, 0.21 mmol, 0.95 equiv) was added to a solution of **4b** (0.100 g, 0.22 mmol, 1 equiv) in MeCN (2 mL). The vial was sealed and heated to 135°C overnight. The resulting red solution was allowed to cool and was filtrated through celite. The solvent was evaporated under vacuum and the residue was extracted with toluene (2 x 5 mL). After removal of the solvent the formed solid was washed with *n*-pentane (5 mL) and dried under vacuum (0.059 g, 42 %).

^1H NMR (400 MHz, CD_2Cl_2 , 25°C): $\delta = 7.66 - 7.58$ (m, 2H, Ph), 7.51 – 7.43 (m, 3H, Ph), 6.64 (s, 1H, Pyrim-H), 3.06 (d, $J = 1.3$ Hz, 3H, N- CH_3), 3.03 (d, $J = 3.0$ Hz, 3H, N- CH_3), 2.57 – 2.43 (m, 2H, $\text{CH}(\text{CH}_3)_2$), 2.24 – 2.13 (m, 2H, $\text{CH}(\text{CH}_3)_2$), 1.42 – 0.80 (m, 24H, $\text{CH}(\text{CH}_3)_2$).

$^{31}\text{P}\{^1\text{H}\}$ NMR (162 MHz, CD_2Cl_2 , 25°C): $\delta = 132.2, 71.8$ ppm.

IR (ATR, cm^{-1}): 2010 (ν_{CO}), 1876 (ν_{CO}), 1837 (ν_{CO}).

[W(κ^2 -*P,N*-phenyl-pyrimidine)(CO)₄] (12)



In a microwave glass vial W(CO)_6 (0.075 g, 0.21 mmol, 0.95 equiv) was added to a solution of **4b** (0.100 g, 0.22 mmol, 1 equiv) in MeCN (2 mL). The vial was sealed and heated to 135°C overnight. The resulting orange solution was allowed to cool and was filtrated through celite. The solvent was evaporated under vacuum and the residue was washed with *n*-pentane (3 mL) to yield a yellow solid (0.091 g, 57 %).

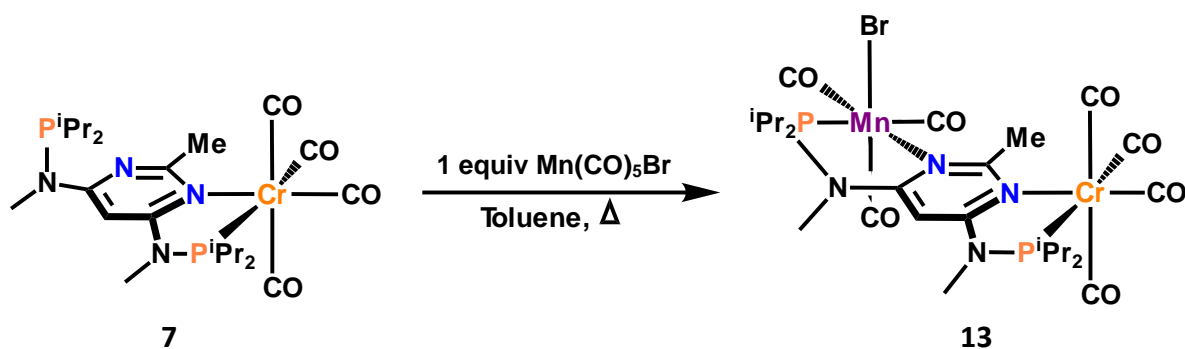
^1H NMR (400 MHz, CD_2Cl_2 , 25°C): δ = 7.67 – 7.34 (m, 5H, Ph), 6.67 (s, 1H, Pyrim-H), 3.14 – 2.90 (m, 6H, N- CH_3), 2.60 – 2.44 (m, 2H, $\text{CH}(\text{CH}_3)_2$), 2.24 – 2.12 (m, 2H, $\text{CH}(\text{CH}_3)_2$), 1.47 – 0.84 (m, 24H, $\text{CH}(\text{CH}_3)_2$) ppm.

$^{31}\text{P}\{^1\text{H}\}$ NMR (162 MHz, CD_2Cl_2 , 25°C): δ = 124.4, 72.1 ppm.

IR (ATR, cm^{-1}): 2005 (ν_{CO}), 1864 (ν_{CO}), 1829 (ν_{CO}).

5.3.2 Synthesis of Binuclear Complexes

$[\mu^2$ -(κ^2 -*P,N*-methyl-pyrimidine){Cr(CO)₄Mn(CO)₃Br}] (13)



In a Schlenk flask $\text{Mn(CO)}_5\text{Br}$ (0.040 g, 0.15 mmol, 1 equiv) was added to a solution **7** (0.080 g, 0.15 mmol, 1 equiv) in toluene (5 mL). Upon heating to reflux, the solution turned orange and CO gas emission was observed. The mixture was refluxed for ten minutes until no further gas emission occurred. Solvent volume was reduced to a third under vacuum and *n*-pentane (7 mL) was added slowly. After sedimentation the clear solution was decanted off and the

formed precipitate was washed with *n*-pentane (7 mL). After drying under vacuum the product was obtained as a yellow solid (0.083 g, 74 %).

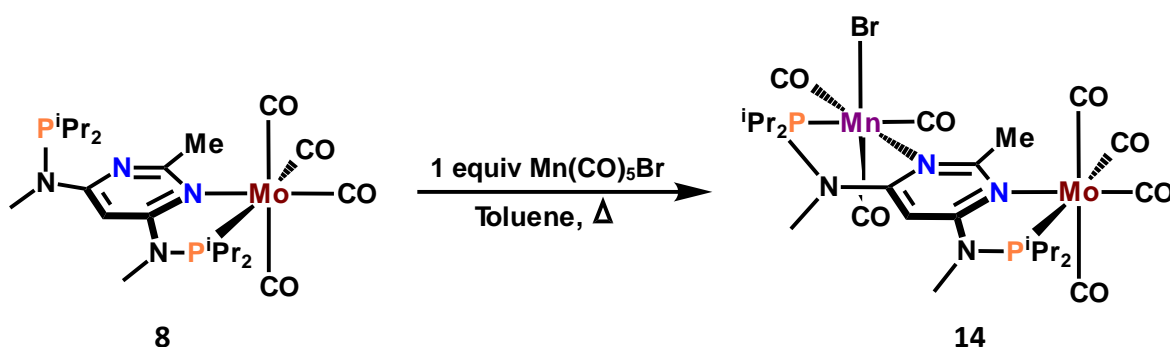
^1H NMR (600 MHz, CD_2Cl_2 , 25°C): δ = 5.49 (s, 1H, Pyrim-H), 3.46 (s, 3H, Me), 3.12 (s, 3H, N-CH₃), 3.04 (s, 3H, N-CH₃), 2.76 (s, 2H, $\text{CH}(\text{CH}_3)_2$), 2.60 (s, 2H, $\text{CH}(\text{CH}_3)_2$), 1.68 – 1.02 (m, 24H, $\text{CH}(\text{CH}_3)_2$) ppm.

$^{13}\text{C}\{^1\text{H}\}$ NMR (151 MHz, CD_2Cl_2 , 25°C): δ = 229.2 (d, J = 13.9 Hz, CO), 224.8 (CO), 223.9 (d, J = 20.2 Hz, CO), 222.7 (CO), 220.2 (d, J = 13.9 Hz, CO), 219.5 (d, J = 13.9 Hz, CO), 214.9 (d, J = 36.4 Hz, CO), 174.4 (Pyrim-C²), 167.8 (d, J = 15.0 Hz, Pyrim-C^{4/6}), 167.6 (d, J = 14.4 Hz, Pyrim-C^{4/6}), 83.7 (t, J = 5.5 Hz, Pyrim-C⁵), 38.7 (Me), 35.3 (d, J = 6.9 Hz, N-CH₃), 34.4 (d, J = 6.4 Hz, N-CH₃), 32.56 – 29.63 (m, $\text{CH}(\text{CH}_3)_2$), 19.7 – 17.8 (m, $\text{CH}(\text{CH}_3)_2$) ppm.

$^{31}\text{P}\{^1\text{H}\}$ NMR (243 MHz, CD_2Cl_2 , 25°C): δ = 154.0, 144.7 ppm.

IR (ATR, cm^{-1}): 2020 (ν_{CO}), 2005 (ν_{CO}), 1880 (ν_{CO}), 1821 (ν_{CO}).

$[\mu^2-(\kappa^2\text{-}P,N\text{-methyl-pyrimidine})\{\text{Mo}(\text{CO})_4\text{Mn}(\text{CO})_3\text{Br}\}]$ (14)



In a Schlenk flask $\text{Mn}(\text{CO})_5\text{Br}$ (0.046 g, 0.17 mmol, 1 equiv) was added to a solution of **8** (0.100 g, 0.17 mmol, 1 equiv) in toluene (5 mL). Upon heating to reflux, the solution turned orange and CO gas emission was observed. The mixture was refluxed for ten minutes until no further gas emission occurred. The solvent was removed under vacuum and the formed precipitate was washed with *n*-pentane (7 mL). After drying under vacuum the product was obtained as a yellow solid (0.109 g, 79 %).

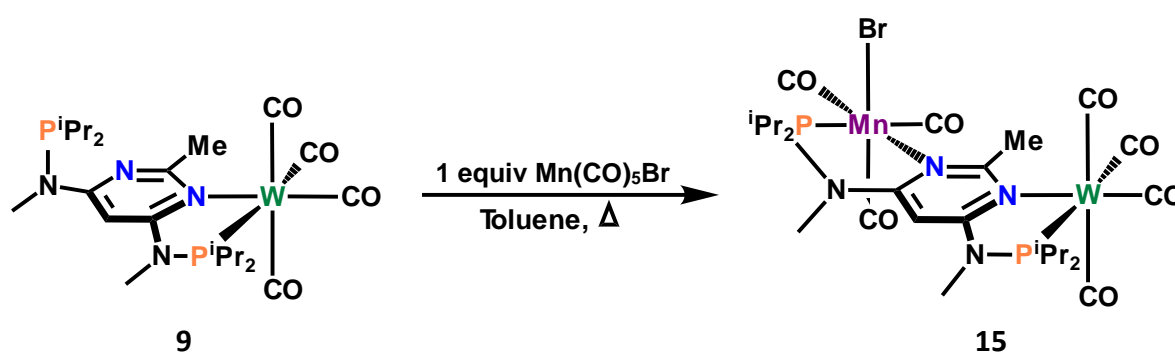
^1H NMR (600 MHz, CD_2Cl_2 , 25°C): δ = 5.54 (s, 1H, Pyrim-H), 3.45 (s, 3H, Me), 3.13 (s, 3H, N-CH₃), 3.04 (s, 3H, N-CH₃), 2.78 (s, 2H, $\text{CH}(\text{CH}_3)_2$), 2.49 (s, 2H, $\text{CH}(\text{CH}_3)_2$), 1.62 – 1.00 (m, 24H, $\text{CH}(\text{CH}_3)_2$) ppm.

$^{13}\text{C}\{^1\text{H}\}$ NMR (151 MHz, CD_2Cl_2 , 25°C): $\delta = 223.9$ (d, $J = 24.1$ Hz, CO), 222.5 (d, $J = 18.8$ Hz, CO), 221.8 (d, $J = 8.7$ Hz, CO), 214.9 (d, $J = 39.3$ Hz, CO), 214.3 (d, $J = 36.4$ Hz, CO), 209.2 (d, $J = 9.8$ Hz, CO), 208.5 (d, $J = 9.2$ Hz, CO), 173.6 (t, $J = 2.7$ Hz, Pyrim- C^2), 167.9 (d, $J = 14.3$ Hz, Pyrim- $\text{C}^{4/6}$), 167.6 (d, $J = 14.0$ Hz, Pyrim- $\text{C}^{4/6}$), 84.1 (t, $J = 5.3$ Hz, Pyrim- C^5), 39.6 (Me), 35.30 (d, $J = 6.3$ Hz, N- CH_3), 34.76 (d, $J = 5.1$ Hz, N- CH_3), $32.02 - 29.75$ (m, $\underline{\text{C}}\text{H}(\text{CH}_3)_2$), $19.93 - 17.54$ (m, $\text{CH}(\underline{\text{C}}\text{H}_3)_2$) ppm.

$^{31}\text{P}\{^1\text{H}\}$ NMR (243 MHz, CD_2Cl_2 , 25°C): $\delta = 145.2$, 138.2 ppm.

IR (ATR, cm^{-1}): 2014 (ν_{CO}), 1882 (ν_{CO}), 1841 (ν_{CO}).

$[\mu^2-(\kappa^2\text{-}P,N\text{-methyl-pyrimidine})\{\text{W}(\text{CO})_4\text{Mn}(\text{CO})_3\text{Br}\}]$ (15)



In a Schlenk flask $\text{Mn}(\text{CO})_5\text{Br}$ (0.019 g, 0.07 mmol, 1 equiv) was added to a solution of **9** (0.047 g, 0.07 mmol, 1 equiv) in toluene (5 mL). Upon heating to reflux, the solution turned orange and CO gas emission was observed. The mixture was refluxed for ten minutes until no further gas emission occurred. The solvent was removed under vacuum and the formed precipitate was washed with *n*-pentane (2 x 7 mL). After drying under vacuum the product was obtained as a yellow solid (0.045 g, 71 %).

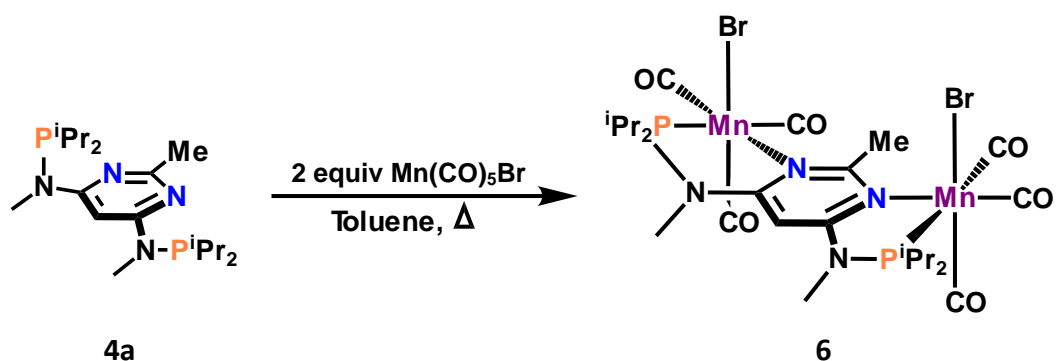
^1H NMR (600 MHz, CD_2Cl_2 , 25°C): $\delta = 5.56$ (s, 1H, Pyrim-H), 3.53 (s, 3H, Me), 3.15 (s, 3H, N- CH_3), 3.05 (s, 3H, N- CH_3), 2.79 (s, 2H, $\underline{\text{C}}\text{H}(\text{CH}_3)_2$), $2.59 - 2.43$ (m, 2H, $\text{CH}(\text{CH}_3)_2$), $1.60 - 0.95$ (m, 24H, $\text{CH}(\underline{\text{C}}\text{H}_3)_2$) ppm.

$^{13}\text{C}\{^1\text{H}\}$ NMR (151 MHz, CD_2Cl_2 , 25°C): $\delta = 223.9$ (d, $J = 21.1$ Hz, CO), 222.5 (d, $J = 15.9$ Hz, CO), 214.9 (d, $J = 36.2$ Hz, CO), 210.6 (d, $J = 4.8$ Hz, CO), 208.2 (d, $J = 35.4$ Hz, CO), 203.5 (d, $J = 7.5$ Hz, CO), 202.8 (d, $J = 7.5$ Hz, CO), 174.2 (t, $J = 3.1$ Hz, Pyrim- C^2), 168.9 (d, $J = 13.6$ Hz, Pyrim- $\text{C}^{4/6}$), 167.4 (d, $J = 13.8$ Hz, Pyrim- $\text{C}^{4/6}$), 84.1 (t, $J = 5.2$ Hz, Pyrim- C^5), 40.9 (Me), 35.47 (d, $J = 6.3$ Hz, N- CH_3), 35.2 (d, $J = 4.6$ Hz, N- CH_3), $32.7 - 29.8$ (m, $\underline{\text{C}}\text{H}(\text{CH}_3)_2$), $20.0 - 17.7$ (m, $\text{CH}(\underline{\text{C}}\text{H}_3)_2$).

$^{31}\text{P}\{^1\text{H}\}$ NMR (243 MHz, CD_2Cl_2 , 25°C): $\delta = 145.4, 130.5$ (t, $J = 126.7$ Hz) ppm.

IR (ATR, cm^{-1}): 2010 (ν_{CO}), 1874 (ν_{CO}), 1835 (ν_{CO}).

$[\mu^2-(\kappa^2\text{-}P,N\text{-methyl-pyrimidine})\{\text{Mn}(\text{CO})_3\text{Br}\}_2]$ (6)



In a Schlenk flask $\text{Mn}(\text{CO})_5\text{Br}$ (0.286 g, 1.04 mmol, 2 equiv) was added to a solution of **4a** (0.200 g, 0.52 mmol, 1 equiv) in toluene (10 mL). Upon heating to reflux, the solution turned orange and CO gas emission was observed. The mixture was refluxed for ten minutes until no further gas emission occurred. The solvent was removed under vacuum and the formed precipitate was washed with *n*-pentane (4 mL). After drying under vacuum the product was obtained as a yellow solid (0.371 g, 86 %).

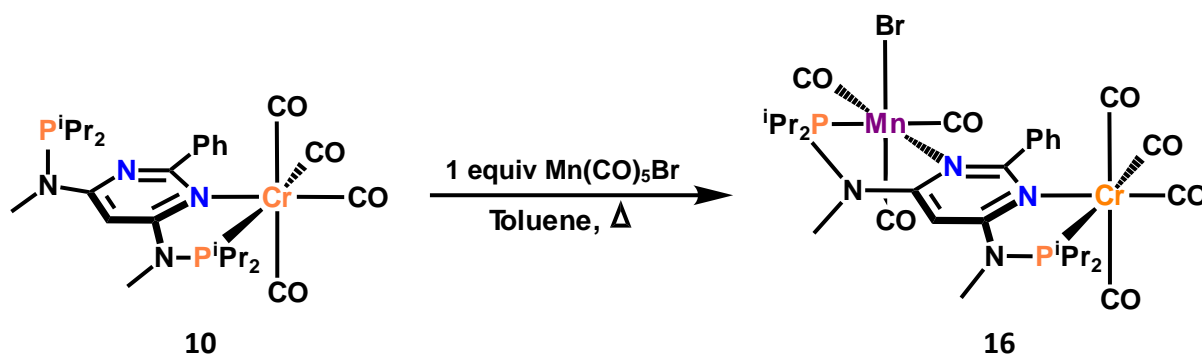
^1H NMR (600 MHz, CD_2Cl_2 , 25°C): $\delta = 5.61$ (s, 1H, Pyrim-H), 3.65 (d, $J = 5.7$ Hz, 3H, Me), 3.15 (s, 6H, N-CH₃), 2.95 (s, 2H, $\underline{\text{C}}\text{H}(\text{CH}_3)_2$), 2.79 (s, 2H, $\underline{\text{C}}\text{H}(\text{CH}_3)_2$), 1.77 – 1.02 (m, 24H, CH($\underline{\text{C}}\text{H}_3$)₂) ppm.

$^{13}\text{C}\{^1\text{H}\}$ NMR (151 MHz, CD_2Cl_2 , 25°C): $\delta = 224.0$ (d, $J = 25.5$ Hz, CO), 222.2 (CO), 214.9 (d, $J = 39.4$ Hz, CO), 174.3 (Pyrim-C²), 174.1 (Pyrim-C²), 168.1 (Pyrim-C^{4/6}), 168.0 (Pyrim-C^{4/6}), 167.9 (Pyrim-C^{4/6}), 85.1 (t, $J = 5.8$ Hz, Pyrim-C⁵), 84.7 (t, $J = 4.7$ Hz, Pyrim-C⁵), 37.9 (Me), 37.7 (Me), 35.7 (d, $J = 6.1$ Hz, N-CH₃), 35.5 (d, $J = 6.1$ Hz, N-CH₃), 32.0 – 31.5 (m, $\underline{\text{C}}\text{H}(\text{CH}_3)_2$), 30.4 – 29.5 (m, $\underline{\text{C}}\text{H}(\text{CH}_3)_2$), 22.0 – 17.3 (m, CH($\underline{\text{C}}\text{H}_3$)₂) ppm.

$^{31}\text{P}\{^1\text{H}\}$ NMR (243 MHz, CD_2Cl_2 , 25°C): $\delta = 146.7, 145.8$ ppm.

IR (ATR, cm^{-1}): 2020 (ν_{CO}), 1934 (ν_{CO}), 1907 (ν_{CO}).

$[\mu^2-(\kappa^2-P,N\text{-phenyl-pyrimidine})\{\text{Cr}(\text{CO})_4\text{Mn}(\text{CO})_3\text{Br}\}]$ (16)



In a Schlenk flask $\text{Mn}(\text{CO})_5\text{Br}$ (0.020 g, 0.07 mmol, 0.95 equiv) was added to a solution of **10** (0.048 g, 0.08 mmol, 1 equiv) in toluene (5 mL). Upon heating to reflux, the solution turned orange and CO gas emission was observed. The mixture was refluxed for ten minutes until no further gas emission occurred. The solvent was removed under vacuum and the formed precipitate was washed with *n*-pentane (2 x 7 mL). After drying under vacuum the product was obtained as a yellow solid (0.039 g, 63 %).

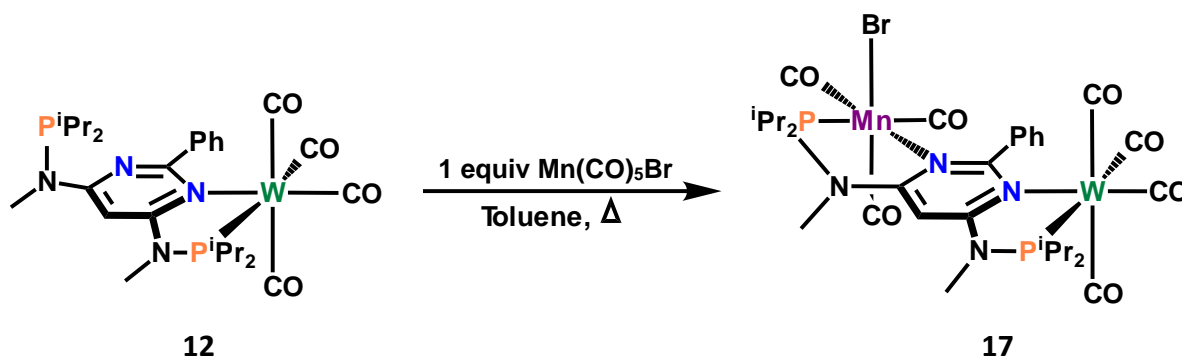
^1H NMR (600 MHz, CD_2Cl_2 , 25°C): δ = 7.73 – 7.53 (m, 5H, Ph), 5.64 (s, 1H, Pyrim-H), 3.19 (s, 3H, N- CH_3), 3.08 (d, J = 17.5 Hz, 3H, N- CH_3), 3.00 – 2.43 (m, 4H, $\text{CH}(\text{CH}_3)_2$), 1.66 – 1.08 (m, 24H, $\text{CH}(\text{CH}_3)_2$) ppm.

$^{13}\text{C}\{^1\text{H}\}$ NMR (151 MHz, CD_2Cl_2 , 25°C): δ = 229.7 (d, J = 13.2 Hz, CO), 224.5 (d, J = 24.7 Hz, CO), 220.4 (dd, J = 13.4, 7.7 Hz, CO), 219.1 (d, J = 4.7 Hz, C=), 208.7 (d, J = 39.5 Hz, CO), 173.71 (Pyrim- C^2), 168.7 (m, Pyrim- $\text{C}^{4/6}$), 145.2 (Ph- C^1) 131.6 – 129.3 (s/s/s/s, Ph), 85.7 (t, J = 5.4 Hz, Pyrim- C^5), 35.8 (d, J = 6.4 Hz, N- CH_3), 34.7 (d, J = 6.1 Hz, N- CH_3), 32.3 – 30.0 (m/d, J = 20.2 Hz/d, J = 19.4 Hz, $\text{CH}(\text{CH}_3)_2$), 20.2 – 17.2 (m, $\text{CH}(\text{CH}_3)_2$) ppm.

$^{31}\text{P}\{^1\text{H}\}$ NMR (243 MHz, CD_2Cl_2 , 25°C): δ = 151.4, 143.2 ppm.

IR (ATR, cm^{-1}): 2020 (ν_{CO}), 2005 (ν_{CO}), 1880 (ν_{CO}), 1821 (ν_{CO}).

[μ^2 -(κ^2 -*P,N*-phenyl-pyrimidine){W(CO)₄Mn(CO)₃Br}] (17)



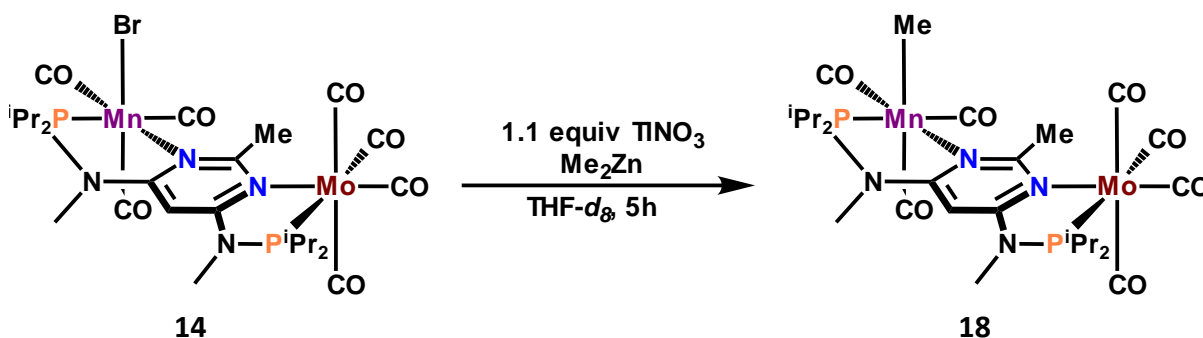
In a Schlenk flask Mn(CO)₅Br (0.020 g, 0.07 mmol, 0.95 equiv) was added to a solution of **12** (0.048 g, 0.08 mmol, 1 equiv) in toluene (5 mL). Upon heating to reflux, the solution turned orange and CO gas emission was observed. The mixture was refluxed for ten minutes until no further gas emission occurred. The solvent was removed under vacuum and the formed precipitate was stirred with *n*-pentane (3 mL) overnight. After decantation of *n*-pentane and drying under vacuum the product was obtained as a yellow solid (0.084 g, 70 %).

³¹P NMR (162 MHz, CD₂Cl₂, 25°C): δ = 144.1, 127.9 (t, *J* = 128.9 Hz) ppm.

IR (ATR, cm⁻¹): 2022 (ν_{CO}), 2009 (ν_{CO}), 1898 (ν_{CO}), 1856 (ν_{CO}).

5.4 Functionalization of Complexes

[μ^2 -(κ^2 -*P,N*-phenyl-pyrimidine){Mo(CO)₄Mn(CO)₃Me}] (18)

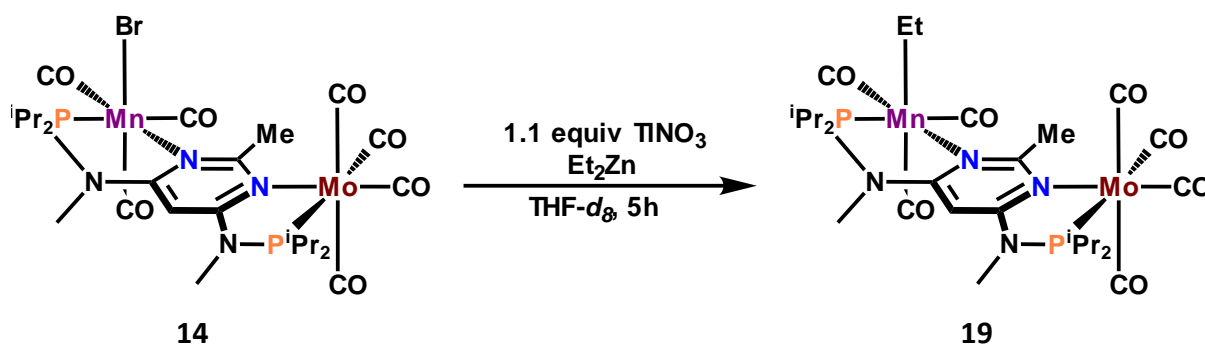


A screw cap vial (8 mL) was charged with **14** (0.05 g, 0.06 mmol, 1 equiv), TINO₃ (0.018 g, 0.07 mmol, 1.1 equiv) and THF-*d*₈ (0.8 mL). After addition of Me₂Zn (10 % in hexane, 0.15 mL) the suspension was stirred at room temperature. After 5 hours the orange suspension was filtered into an NMR tube.

^1H NMR (400 MHz, THF- d_8 , 25°C): δ = 5.54 (s, 1H, Pyrim-H), 3.43 (s, 3H, Me), 3.13 (s, 3H, N-CH₃), 2.99 (s, 3H, N-CH₃), 2.92 (s, 2H, $\underline{\text{C}}\text{H}(\text{CH}_3)_2$), 2.42 (s, 2H, $\underline{\text{C}}\text{H}(\text{CH}_3)_2$), 1.82 – 0.52 (m, 24H, CH($\underline{\text{C}}\text{H}_3$)₂), -1.03 (s, 3H, Me-Mn) ppm.

^{31}P NMR (162 MHz, THF- d_8 , 25°C): δ = 157.6, 137.2 ppm.

$[\mu^2-(\kappa^2\text{-}P,N\text{-phenyl-pyrimidine})\{\text{Mo}(\text{CO})_4\text{Mn}(\text{CO})_3\text{Et}\}]$ (19)

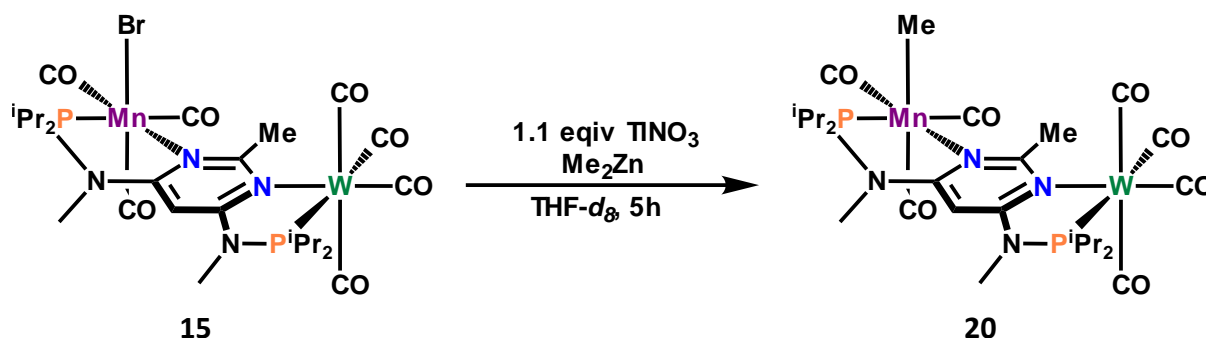


A screw cap vial (8 mL) was charged with **14** (0.05 g, 0.06 mmol, 1 equiv), TiNO₃ (0.018 g, 0.07 mmol, 1.1 equiv) and THF- d_8 (0.8 mL). After addition of Et₂Zn (15 w% in hexane, 0.15 mL) the suspension was stirred at room temperature. After 5 hours the brown suspension was filtered into an NMR tube.

^1H NMR (400 MHz, THF- d_8 , 25°C): δ = 5.52 (s, 1H, Pyrim-H), 3.48 (s, 3H, Me), 3.12 – 3.06 (m, 3H, N-CH₃), 3.06 (s, 3H, N-CH₃), 3.01 – 2.87 (m, 2H, $\underline{\text{C}}\text{H}(\text{CH}_3)_2$), 2.49 – 2.37 (m, 2H, $\underline{\text{C}}\text{H}(\text{CH}_3)_2$), 1.57 – 0.54 (m, 24H, CH($\underline{\text{C}}\text{H}_3$)₂), 0.18 – 0.07 (m, 2H, CH₃ $\underline{\text{C}}\text{H}_2$ -Mn), -0.58 (t, J = 8.8 Hz, 3H, $\underline{\text{C}}\text{H}_3\text{CH}_2$ -Mn) ppm.

^{31}P NMR (162 MHz, THF- d_8 , 25°C): δ = 179.0, 136.0 ppm.

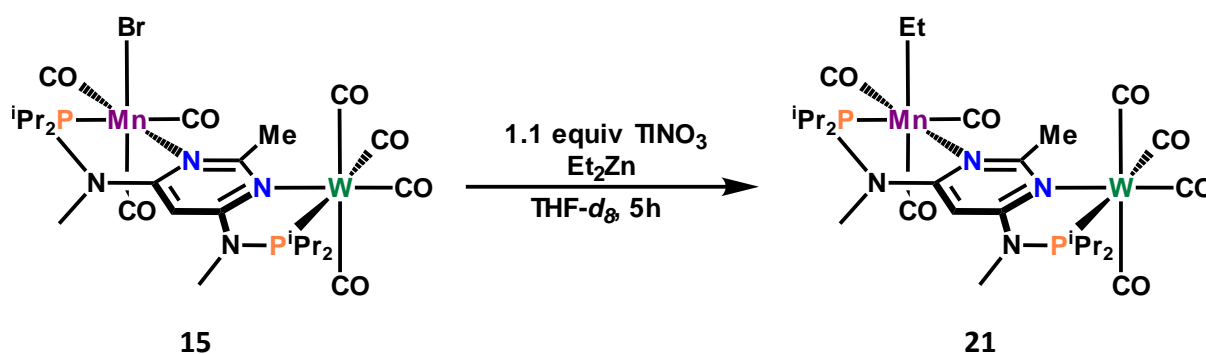
$[\mu^2-(\kappa^2-P,N\text{-phenyl-pyrimidine})\{W(CO)_4Mn(CO)_3Me\}]$ (20)



A screw cap vial (8 mL) was charged with **15** (0.05 g, 0.06 mmol, 1 equiv), TiNO_3 (0.018 g, 0.07 mmol, 1.1 equiv) and $\text{THF-}d_8$ (0.8 mL). After addition of Me_2Zn (10 w% in hexane, 0.15 mL) the suspension was stirred at room temperature. After 5 hours the orange suspension was filtered into an NMR tube.

^{31}P NMR (162 MHz, $\text{THF-}d_8$, 25°C): $\delta = 157.8, 129.4$ ppm.

$[\mu^2-(\kappa^2-P,N\text{-phenyl-pyrimidine})\{W(CO)_4Mn(CO)_3Me\}]$ (21)



A screw cap vial (8 mL) was charged with **15** (0.05 g, 0.06 mmol, 1 equiv), TiNO_3 (0.018 g, 0.07 mmol, 1.1 equiv) and $\text{THF-}d_8$ (0.8 mL). After addition of Et_2Zn (15 w% in hexane, 0.15 mL) the suspension was stirred at room temperature. After 5 hours the dark brown suspension was filtered into an NMR tube.

^{31}P NMR (162 MHz, $\text{THF-}d_8$, 25°C): $\delta = 179.7, 128.4$ ppm.

6 References

- (1) Armor, J. N. A History of Industrial Catalysis. *Catal. Today* **2011**, *163*, 3–9.
- (2) *Critical Raw Materials for the EU, Report of the Ad-Hoc Working Group on Defining Critical Raw Materials.*; European Commission: Enterprise and Industry; 39; European Commission, 2010; pp 1–84.
- (3) Haynes, W. M. *CRC Handbook of Chemistry and Physics*, 97th Edition.; CRC Press, 2016.
- (4) Hartwig, J. F. *Organotransition Metal Chemistry: From Bonding to Catalysis*; University Science Books: Mill Valley, CA, 2010.
- (5) Crabtree, R. H. *The Organometallic Chemistry of the Transition Metals*, 6th ed.; Wiley & Sons, Inc, John Wiley & Sons, Incorporated, Wiley-Blackwell: New York, 2019.
- (6) Lewis, K. E.; Golden, D. M.; Smith, G. P. Organometallic Bond Dissociation Energies: Laser Pyrolysis of Iron Pentacarbonyl, Chromium Hexacarbonyl, Molybdenum Hexacarbonyl, and Tungsten Hexacarbonyl. *J. Am. Chem. Soc.* **1984**, *106*, 3905–3912.
- (7) Elschenbroich, C. *Organometallic Chemie*, 6., überarb. Aufl.; Teubner Studienbücher Chemie; Teubner: Wiesbaden, 2008.
- (8) Coe, B. J.; Glenwright, S. J. Trans-Effects in Octahedral Transition Metal Complexes. *Coord. Chem. Rev.* **2000**, *203*, 5–80.
- (9) Sugahara, T.; Ferao, A. E.; Planells, A. R.; Guo, J.-D.; Aoyama, S.; Igawa, K.; Tomooka, K.; Sasamori, T.; Hashizume, D.; Nagase, S.; Tokitoh, N. 1,2-Insertion Reactions of Alkynes into Ge–C Bonds of Arylbromogermylene. *Dalton Trans.* **2020**, *49*, 7189–7196.
- (10) Shusterman, A. J.; Tamir, I.; Pross, A. The Mechanism of Organometallic Migration Reactions. A Configuration Mixing (CM) Approach. *J. Organomet. Chem.* **1988**, *340*, 203–222.
- (11) Calderazzo, F.; Cotton, F. A. Carbon Monoxide Insertion Reactions. I. The Carbonylation of Methyl Manganese Pentacarbonyl and Decarbonylation of Acetyl Manganese Pentacarbonyl. *Inorg. Chem.* **1962**, *1*, 30–36.
- (12) Calderazzo, F. Synthetic and Mechanistic Aspects of Inorganic Insertion Reactions. Insertion of Carbon Monoxide. *Angew. Chem. Int. Ed. Engl.* **1977**, *16*, 299–311.
- (13) Lau, K. S. Y.; Becker, Y.; Huang, F.; Baenziger, N.; Stille, J. K. Mechanism of Decarbonylation of Acid Chlorides with Chlorotris(Triphenylphosphine)Rhodium(I) Structure and Stereochemistry. *J. Am. Chem. Soc.* **1977**, *99*, 5664–5672.
- (14) Hitam, R. B.; Narayanaswamy, R.; Rest, A. J. Matrix Isolation Studies of the Bonding of Acetyl Groups in the Co-Ordinatively Unsaturated Species Acetyltetracarbonylmanganese and Acetylmonocarbonyl(η -Cyclopentadienyl)Iron. *J. Chem. Soc. Dalton Trans.* **1983**, 615–618.
- (15) Derecskei-Kovacs, A.; Marynick, D. S. A New Look at an Old Reaction: The Potential Energy Surface for the Thermal Carbonylation of Mn(CO)₅CH₃. The Role of Two Energetically Competitive Intermediates on the Reaction Surface, and Comments on the Photodecarbonylation of Mn(CO)₅(COCH₃). *J. Am. Chem. Soc.* **2000**, *122*, 2078–2086.
- (16) Zhou, T.; Malakar, S.; Webb, S. L.; Krogh-Jespersen, K.; Goldman, A. S. Polar Molecules Catalyze CO Insertion into Metal-Alkyl Bonds through the Displacement of an Agostic C–H Bond. *Proc. Natl. Acad. Sci. U. S. A.* **2019**, *116*, 3419–3424.
- (17) Butts, S. B.; Richmond, T. G.; Shriver, D. F. Acceleration of the Methyl Migration Reaction with Proton Acids. *Inorg. Chem.* **1981**, *20*, 278–280.
- (18) Blanco-Urgoiti, J.; Añorbe, L.; Pérez-Serrano, L.; Domínguez, G.; Pérez-Castells, J. The Pauson–Khand Reaction, a Powerful Synthetic Tool for the Synthesis of Complex Molecules. *Chem. Soc. Rev.* **2004**, *33*, 32–42.

- (19) Pauson, P. L.; Khand, I. U. Uses of Cobalt-Carbonyl Acetylene Complexes in Organic Synthesis. *Ann. N. Y. Acad. Sci.* **1977**, *295*, 2–14.
- (20) Sugihara, T.; Yamada, M.; Yamaguchi, M.; Nishizawa, M. The Intra- and Intermolecular Pauson-Khand Reaction Promoted by Alkyl Methyl Sulfides. *Synlett* **1999**, *6*, 771–773.
- (21) Jeong, N.; Hwang, S. H.; Lee, Y.; Chung, Y. K. Catalytic Version of the Intramolecular Pauson-Khand Reaction. *J. Am. Chem. Soc.* **1994**, *116*, 3159–3160.
- (22) Neto, D. H. C.; Santos, A. A. M. D.; Silva, J. C. S. D.; Rocha, W. R.; Dias, R. P. Propene Hydroformylation Reaction Catalyzed by HRh(CO)(BISBI): A Thermodynamic and Kinetic Analysis of the Full Catalytic Cycle. *Eur. J. Inorg. Chem.* **2020**, *2020*, 3907–3916.
- (23) Slauch, L. H.; Mullineaux, R. D. Novel Hydroformylation Catalysts. *J. Organomet. Chem.* **1968**, *13*, 469–477.
- (24) Heck, R. F.; Breslow, D. S. The Reaction of Cobalt Hydrotetracarbonyl with Olefins. *J. Am. Chem. Soc.* **1961**, *83*, 4023–4027.
- (25) Osborn, J. A.; Jardine, F. H.; Young, J. F.; Wilkinson, G. The Preparation and Properties of Tris(Triphenylphosphine)Halogenorhodium(I) and Some Reactions Thereof Including Catalytic Homogeneous Hydrogenation of Olefins and Acetylenes and Their Derivatives. *J. Chem. Soc. Inorg. Phys. Theor.* **1966**, 1711–1732.
- (26) Jones, J. H. The Cativa™ Process for the Manufacture of Acetic Acid. *Platin. Met. Rev* **2000**, *44*, 94.
- (27) Tolman, C. A. Steric Effects of Phosphorus Ligands in Organometallic Chemistry and Homogeneous Catalysis. *Chem. Rev.* **1977**, *77*, 313–348.
- (28) Vaska, L.; DiLuzio, J. W. Activation of Hydrogen by a Transition Metal Complex at Normal Conditions Leading to a Stable Molecular Dihydride. *J. Am. Chem. Soc.* **1962**, *84*, 679–680.
- (29) Gensow, M.-N. B.; Freixa, Z.; Leeuwen, P. W. N. M. van. Bite Angle Effects of Diphosphines in C–C and C–X Bond Forming Cross Coupling Reactions. *Chem. Soc. Rev.* **2009**, *38*, 1099–1118.
- (30) Goertz, W.; Keim, W.; Vogt, D.; Englert, U.; Boele, M. D. K.; Veen, L. A. van der; Kamer, P. C. J.; Leeuwen, P. W. N. M. van. Electronic Effects in the Nickel-Catalysed Hydrocyanation of Styrene Applying Chelating Phosphorus Ligands with Large Bite Angles. *J. Chem. Soc. Dalton Trans.* **1998**, 2981–2988.
- (31) Moiseev, D. V.; Malysheva, Y. B.; Shavyrin, A. S.; Kurskii, Y. A.; Gushchin, A. V. Study of Homo- and Cross-Coupling Competition in the Reaction of Triarylbi-muth(V) Dicarboxylates with Methyl Acrylate in the Presence of a Palladium Catalyst. *J. Organomet. Chem.* **2005**, *690*, 3652–3663.
- (32) Casey, C. P.; Whiteker, G. T.; Melville, M. G.; Petrovich, L. M.; Gavney, J. A.; Powell, D. R. Diphosphines with Natural Bite Angles near 120.Degree. Increase Selectivity for n-Aldehyde Formation in Rhodium-Catalyzed Hydroformylation. *J. Am. Chem. Soc.* **1992**, *114*, 5535–5543.
- (33) Seligson, A. L.; Trogler, W. C. Cone Angles for Amine Ligands. X-Ray Crystal Structures and Equilibrium Measurements for Ammonia, Ethylamine, Diethylamine, and Triethylamine Complexes with the [Bis(Dimethylphosphino)Ethane]Methylpalladium(II) Cation. *J. Am. Chem. Soc.* **1991**, *113*, 2520–2527.
- (34) Lindoy, L. F.; Livingstone, S. E. Complexes of Iron(II),Cobalt(II) and Nickel(II) with α -Diimines and Related Bidentate Ligands. *Coord. Chem. Rev.* **1967**, *2*, 173–193.
- (35) Chelucci, G.; Thummel, R. P. Chiral 2,2'-Bipyridines, 1,10-Phenanthrolines, and 2,2':6',2''-Terpyridines: Syntheses and Applications in Asymmetric Homogeneous Catalysis. *Chem. Rev.* **2002**, *102*, 3129–3170.

- (36) Müller, D.; Umbricht, G.; Weber, B.; Pfaltz, A. C₂-Symmetric 4,4',5,5'-Tetrahydrobi(Oxazoles) and 4,4',5,5'-Tetrahydro-2,2'-Methylenebis[Oxazoles] as Chiral Ligands for Enantioselective Catalysis Preliminary Communication. *Helv. Chim. Acta* **1991**, *74*, 232–240.
- (37) Ohkuma, T.; Ooka, H.; Hashiguchi, S.; Ikariya, T.; Noyori, R. Practical Enantioselective Hydrogenation of Aromatic Ketones. *J. Am. Chem. Soc.* **1995**, *117*, 2675–2676.
- (38) Ito, M.; Ootsuka, T.; Watari, R.; Shiibashi, A.; Himizu, A.; Ikariya, T. Catalytic Hydrogenation of Carboxamides and Esters by Well-Defined Cp*Ru Complexes Bearing a Protic Amine Ligand. *J. Am. Chem. Soc.* **2011**, *133*, 4240–4242.
- (39) Espinet, P.; Soulantica, K. Phosphine-Pyridyl and Related Ligands in Synthesis and Catalysis. *Coord. Chem. Rev.* **1999**, *193–195*, 499–556.
- (40) Munzeiwa, W. A.; Omondi, B.; Nyamori, V. O. Architecture and Synthesis of P, N-Heterocyclic Phosphine Ligands. *Beilstein J. Org. Chem.* **2020**, *16*, 362–383.
- (41) Rautenstrauch, V.; Challand, R.; Churlaud, R.; Morris, R. H.; Brazi, E.; Mimoun, H.; Abdur-Rashid, K. Catalytic Hydrogenation Processes. US7317131B2, January 8, 2008.
- (42) Noyori, R.; Ohkuma, T. Asymmetric Catalysis by Architectural and Functional Molecular Engineering: Practical Chemo- and Stereoselective Hydrogenation of Ketones. *Angew. Chem. Int. Ed.* **2001**, *40*, 40–73.
- (43) Abdur-Rashid, K.; Lough, A. J.; Morris, R. H. Ruthenium Dihydride RuH₂(PPh₃)₂((R,R)-Cyclohexyldiamine) and Ruthenium Monohydride RuHCl(PPh₃)₂((R,R)-Cyclohexyldiamine): Active Catalyst and Catalyst Precursor for the Hydrogenation of Ketones and Imines. *Organometallics* **2000**, *19*, 2655–2657.
- (44) Saudan, L. A.; Saudan, C. M.; Debieux, C.; Wyss, P. Dihydrogen Reduction of Carboxylic Esters to Alcohols under the Catalysis of Homogeneous Ruthenium Complexes: High Efficiency and Unprecedented Chemoselectivity. *Angew. Chem. Int. Ed.* **2007**, *46*, 7473–7476.
- (45) Mukherjee, A.; Nerush, A.; Leitus, G.; Shimon, L. J. W.; Ben David, Y.; Espinosa Jalapa, N. A.; Milstein, D. Manganese-Catalyzed Environmentally Benign Dehydrogenative Coupling of Alcohols and Amines to Form Aldimines and H₂: A Catalytic and Mechanistic Study. *J. Am. Chem. Soc.* **2016**, *138*, 4298–4301.
- (46) Mastalir, M.; Glatz, M.; Pittenauer, E.; Allmaier, G.; Kirchner, K. Sustainable Synthesis of Quinolines and Pyrimidines Catalyzed by Manganese PNP Pincer Complexes. *J. Am. Chem. Soc.* **2016**, *138*, 15543–15546.
- (47) Kallmeier, F.; Dudziec, B.; Irrgang, T.; Kempe, R. Manganese-Catalyzed Sustainable Synthesis of Pyrroles from Alcohols and Amino Alcohols. *Angew. Chem. Int. Ed.* **2017**, *56*, 7261–7265.
- (48) Weber, S.; Kirchner, K. The Role of Metal-Ligand Cooperation in Manganese(I)-Catalyzed Hydrogenation/Dehydrogenation Reactions. In *Metal-Ligand Co-operativity: Catalysis and the Pincer-Metal Platform*; van Koten, G., Kirchner, K., Moret, M.-E., Eds.; Topics in Organometallic Chemistry; Springer International Publishing: Cham, 2021; pp 227–261.
- (49) Elangovan, S.; Topf, C.; Fischer, S.; Jiao, H.; Spannenberg, A.; Baumann, W.; Ludwig, R.; Junge, K.; Beller, M. Selective Catalytic Hydrogenations of Nitriles, Ketones, and Aldehydes by Well-Defined Manganese Pincer Complexes. *J. Am. Chem. Soc.* **2016**, *138*, 8809–8814.
- (50) Glatz, M.; Stöger, B.; Himmelbauer, D.; Veiros, L. F.; Kirchner, K. Chemoselective Hydrogenation of Aldehydes under Mild, Base-Free Conditions: Manganese Outperforms Ruthenium. *ACS Catal.* **2018**, *8*, 4009–4016.

- (51) Wei, D.; Bruneau-Voisine, A.; Chauvin, T.; Dorcet, V.; Roisnel, T.; Valyaev, D. A.; Lugan, N.; Sortais, J.-B. Hydrogenation of Carbonyl Derivatives Catalysed by Manganese Complexes Bearing Bidentate Pyridinyl-Phosphine Ligands. *Adv. Synth. Catal.* **2018**, *360*, 676–681.
- (52) Bruneau-Voisine, A.; Wang, D.; Roisnel, T.; Darcel, C.; Sortais, J.-B. Hydrogenation of Ketones with a Manganese PN3P Pincer Pre-Catalyst. *Catal. Commun.* **2017**, *92*, 1–4.
- (53) van Putten, R.; Uslamin, E. A.; Garbe, M.; Liu, C.; Gonzalez-de-Castro, A.; Lutz, M.; Junge, K.; Hensen, E. J. M.; Beller, M.; Lefort, L.; Pidko, E. A. Non-Pincer-Type Manganese Complexes as Efficient Catalysts for the Hydrogenation of Esters. *Angew. Chem. Int. Ed.* **2017**, *56*, 7531–7534.
- (54) Weber, S.; Veiros, L. F.; Kirchner, K. Old Concepts, New Application – Additive-Free Hydrogenation of Nitriles Catalyzed by an Air Stable Alkyl Mn(I) Complex. *Adv. Synth. Catal.* **2019**, *361*, 5412–5420.
- (55) Weber, S.; Brüning, J.; Veiros, L. F.; Kirchner, K. Manganese-Catalyzed Hydrogenation of Ketones under Mild and Base-Free Conditions. *Organometallics* **2021**, Article in press.
- (56) Weber, S.; Stöger, B.; Veiros, L. F.; Kirchner, K. Rethinking Basic Concepts—Hydrogenation of Alkenes Catalyzed by Bench-Stable Alkyl Mn(I) Complexes. *ACS Catal.* **2019**, *9*, 9715–9720.
- (57) Kostera, S.; Weber, S.; Peruzzini, M.; Veiros, L. F.; Kirchner, K.; Gonsalvi, L. Carbon Dioxide Hydrogenation to Formate Catalyzed by a Bench-Stable, Non-Pincer-Type Mn(I) Alkylcarbonyl Complex. *Organometallics* **2021**, Article in press.
- (58) Cotton, F. A. Alkyls And Aryls of Transition Metals. *Chem. Rev.* **1955**, *55*, 551–594.
- (59) Zhou, Y.; Zhang, Y.; Wang, J. Recent Advances in Transition-Metal-Catalyzed Synthesis of Conjugated Enynes. *Org. Biomol. Chem.* **2016**, *14*, 6638–6650.
- (60) Shortland, A. J.; Wilkinson, G. Preparation and Properties of Hexamethyltungsten. *J. Chem. Soc. Dalton Trans.* **1973**, 872–876.
- (61) Kealy, T. J.; Pauson, P. L. A New Type of Organo-Iron Compound. *Nature* **1951**, *168*, 1039–1040.
- (62) Berthold, H. J.; Spiegl, H. J. Über die Bildung von Lithiumtetrachloroferrat(II) Li₂ FeCl₄ bei der Umsetzung von Eisen(III)-chlorid mit Lithiummethyl (1:1) in ätherischer Lösung. *Z. Für Anorg. Allg. Chem.* **1972**, *391*, 193–202.
- (63) Darensbourg, M. York.; Conder, H. L.; Darensbourg, D. J.; Hasday, C. Electronic and Steric Control of Reactions of Benzylmagnesium Chloride with Substituted Metal Carbonyls. *J. Am. Chem. Soc.* **1973**, *95*, 5919–5924.
- (64) Allred, A. L. Electronegativity Values from Thermochemical Data. *J. Inorg. Nucl. Chem.* **1961**, *17*, 215–221.
- (65) Knochel, P. *Organozinc Reagents: A Practical Approach*; The practical approach in chemistry series; Oxford UnivPr: Oxford [u.a.], 1999.
- (66) Santini-Scampucci, C.; Riess, J. G. Preparation of Monomethyl-Niobium(V) and -Tantalum(V) Halides and of Some of Their Complexes. *J. Chem. Soc. Dalton Trans.* **1973**, 2436–2440.
- (67) Fowles, G. W. A.; Rice, D. A.; Wilkins, J. D. Reaction of Dimethylzinc with Tantalum(V) Chloride and Some Co-Ordination Compounds of Methyltantalum(V) Chloride, Dimethyltantalum(V) Chloride and Methylniobium(V) Chloride. *J. Chem. Soc. Dalton Trans.* **1973**, 961–965.
- (68) Moorhouse, S.; Wilkinson, G. Bis[(Trimethylsilyl)Methyl]- and Bis(Neopentyl)-Zinc, and Tris[(Trimethylsilyl)Methyl]Aluminium–Diethyl Ether (1/1); Their Use as Alkylating

- Agents in Forming Niobium and Tantalum Alkyls. *J. Chem. Soc. Dalton Trans.* **1974**, 2187–2190.
- (69) Dilman, A. D.; Levin, V. V. Advances in the Chemistry of Organozinc Reagents. *Tetrahedron Lett.* **2016**, *57*, 3986–3992.
- (70) Tomsu, G. Neue PCP Pincer Pyrimidin Komplexe unedler Übergangsmetalle, Wien, 2017.
- (71) Guram, A. S.; Rennels, R. A.; Buchwald, S. L. A Simple Catalytic Method for the Conversion of Aryl Bromides to Arylamines. *Angew. Chem. Int. Ed. Engl.* **1995**, *34*, 1348–1350.
- (72) Driver, M. S.; Hartwig, J. F. A Rare, Low-Valent Alkylamido Complex, a Diphenylamido Complex, and Their Reductive Elimination of Amines by Three-Coordinate Intermediates. *J. Am. Chem. Soc.* **1995**, *117*, 4708–4709.
- (73) Jones, C. P.; Anderson, K. W.; Buchwald, S. L. Sequential Cu-Catalyzed Amidation-Base-Mediated Camps Cyclization: A Two-Step Synthesis of 2-Aryl-4-Quinolones from *o*-Halophenones. *J. Org. Chem.* **2007**, *72*, 7968–7973.
- (74) Tomsu, G.; Mastalir, M.; Pittenauer, E.; Stöger, B.; Allmaier, G.; Kirchner, K. Ligand-Enforced Switch of the Coordination Mode in Low-Valent Group 6 Carbonyl Complexes Containing Pyrimidine-Based Bisphosphines. *Organometallics* **2018**, *37*, 1919–1926.
- (75) Becker, T. M.; Krause-Bauer, J. A.; Homrighausen, C. L.; Orchin, M. The Preparation and Reactions of the Azides of Fac-Mn(CO)₃(P-P)N₃. The X-Ray Crystal Structures of Fac-[Mn(CO)₃(P-P)(OH₂)]BF₄, Fac-Mn(CO)₃(P-P)(NN₂C(CF₃)N) [(P-P)=dppe and Depe], and Fac-[Mn(CO)₃(Depe)(PPh₃)]BF₄. *Polyhedron* **1999**, *18*, 2563–2571.

7 List of Abbreviations

CO	Carbon monoxide
Cp*	Pentamethylcyclopentadienyl
DCM	Dichloromethane, methylene chloride
Et	Ethyl
Et ₂ Zn	Diethylzinc
HOMO	Highest occupied molecular orbital
ⁱ Pr ₂ PCl	Chlorodiisopropylphosphine
L	Ligand
LUMO	Lowest unoccupied molecular orbital
M	Metal
Me	Methyl
MeCN	Acetonitrile
Mel	Iodomethane
MeLi	Methyl lithium
MeNH ₂	Methylamine
Me-Pyrim	<i>N4,N6</i> -Bis(diisopropylphosphino)- <i>N4,N6,2</i> -trimethylpyrimidine-4,6-diamine
Me ₂ Zn	Dimethylzinc
NaOH	Sodium hydroxide
<i>n</i> BuLi	<i>n</i> Butyllithium
Ph	Phenyl
Ph-Pyrim	<i>N4,N6</i> -bis(diisopropylphosphino)- <i>N4,N6</i> -dimethyl-2-phenylpyrimidine-4,6-diamine
PMe ₃	Trimethylphosphine
POCl ₃	Phosphor(V)oxychloride
Py	Pyridine
<i>t</i> BuNC	<i>t</i> Butyl isocyanide
THF	Tetrahydrofuran